Soft x-ray absorption spectrocopy

Peter Krüger

Graduate School of Advanced Integration Science
Chiba University, Japan

2013.09.16

Outline

Soft X-rays

$100 < h\nu < 3000$ eV $\quad \leftrightarrow \quad 12 > \lambda > 0.4$ nm

penetration depth in condensed matter $< 1\mu$m

Principle of Light absorption

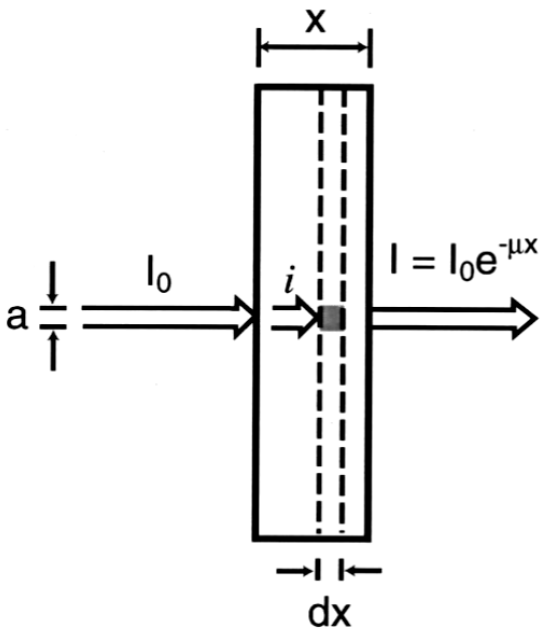

[Rehr Albers RMP 2000]

- incoming flux I_0, after distance x, $I(x)$
- $dI \sim -I(x)dx$ absorbed in $(x, x + dx)$
- $\mu \equiv -dI/Idx$ = absorption coefficient
- $I(x) = I_0 \exp(-\mu x)$ absorption law [Beer-Lambert]
- Absorption spectra = $\mu(\lambda)$.

Absorption edges

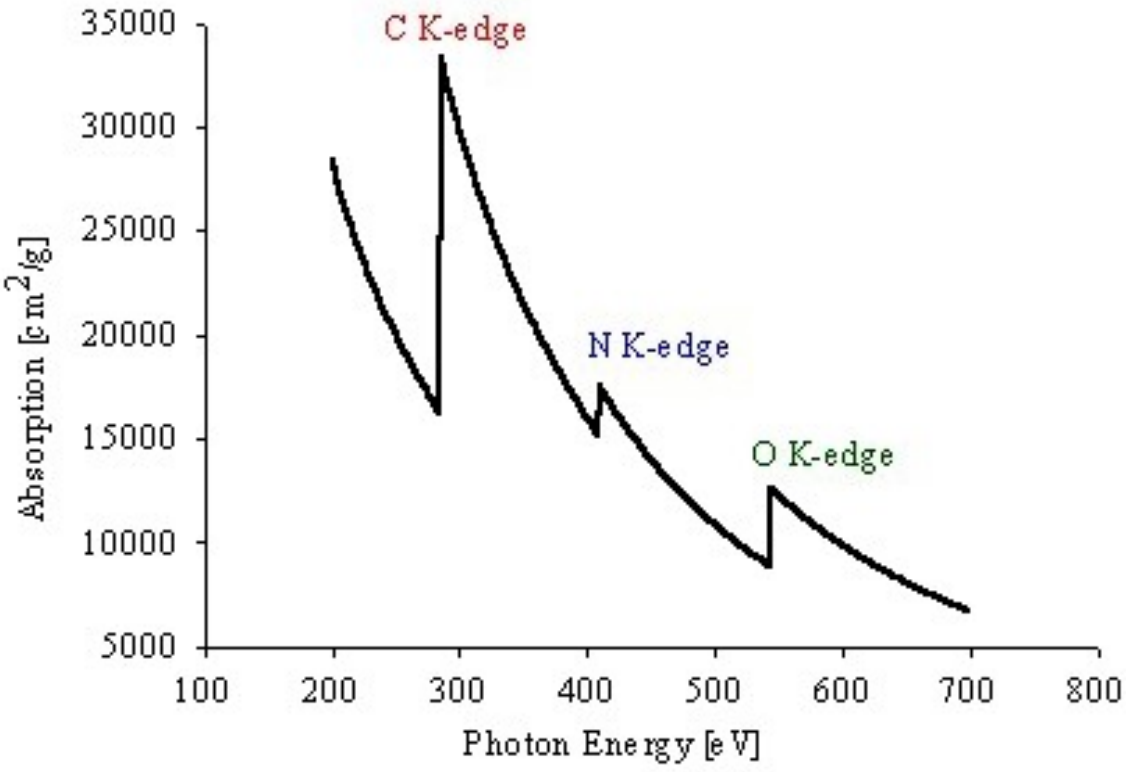

From I. Koprinarov, A. P. Hitchcock

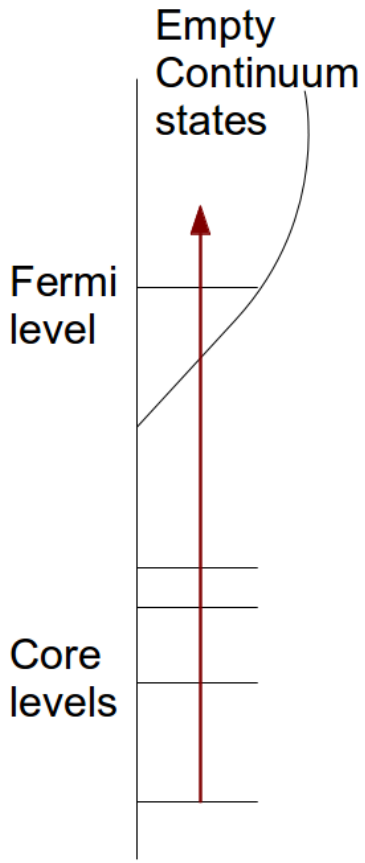

1st row elements: 1s = K-edge, transition metals: 2p = L23-edges, etc

NEXAFS Near-edge x-ray absorption fine structure / XANES X-ray absorption near-edge structure

Chemical analysis. Example: C K-edge of polymers

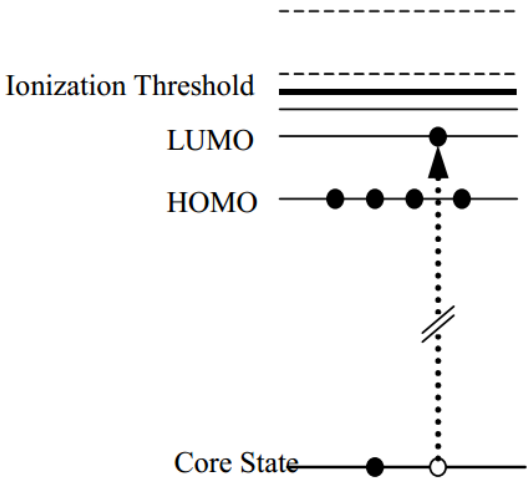

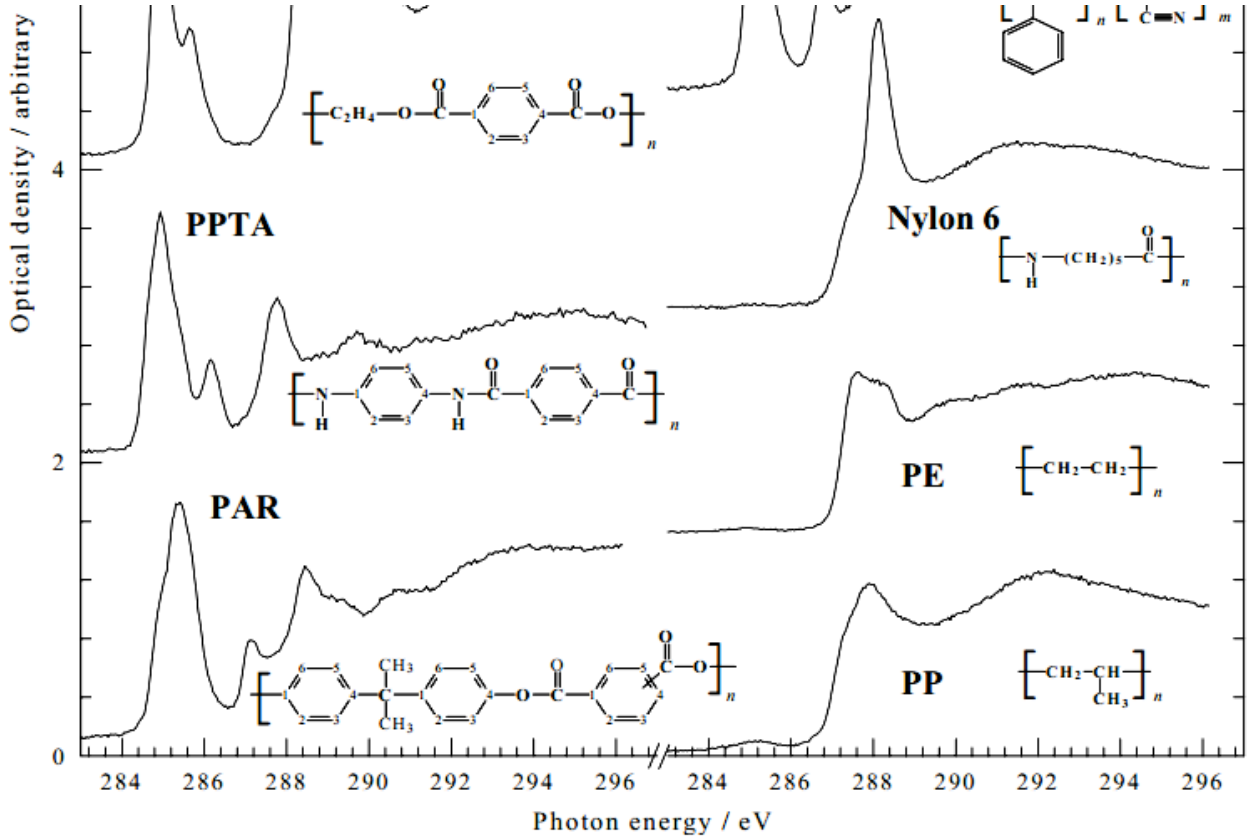

Fig. 3 C 1s NEXAFS spectra of some common polymers. Abbreviation as follows: PC, polycarbonate; PET, poly(ethylene terephthalate); PPTA, poly(p-phenylene terephthalamide); PAR, polyacrylate; PS, polystyrene; SAN, styrene-acrylonitrile; Nylon-6, poly(ε-caprolactam); PP, polypropylene; PE, polyethylene. (Figure adopted from [Ade 97])

From I. Koprinarov, A. P. Hitchcock

Measurement modes

- Transmission.
  Most direct. Correct by definition. Good for hard x-rays.
  Problem: needs homogeneous sample, no thickness variation.
  For soft x-rays, short attenuation length (i.e. μ large), $\rightarrow$ thin samples required, difficult to have no thickness variation.

- FY. Fluorescence yield.
  Decay of core-hole by radiation (fluorescence).
  Number of fluorescence photons measured.
  Bulk sensitive. Liquids, organic matter, high pressure ok.
  But FY small for soft x-rays, where non-radiative (Auger) decay dominates

Measurement modes

- TEY. Total electron yield.
  Most used for soft XAS from solids. Shine on sample.
  Count all photoemitted electrons, most easily from drain current.
  Probing depth limited by electron escape depth $\sim$ 3–10 nm.
  Surface sensitive. Vacuum conditions required.

- PEY. Partial electron yield.
  Measure only a part of the emitted electrons, e.g. number of secondary electron of a certain Auger decay.
  Can yield improved energy resolution and insight into decay process, but PEY may not be exactly proportional to XAS.
  Surface sensitive. High vacuum required.

Theory: Light-Matter interaction

Electronic hamiltonian. Electron operators $\mathbf{r}_i, \mathbf{p}_i$. Nuclei at $\mathbf{R}_j$.

$$H(\{\mathbf{r}_i, \mathbf{p}_i\}) = \sum_i \frac{\mathbf{p}_i^2}{2m} + V(\{\mathbf{r}_i\}, \{\mathbf{R}_j\})$$

X-ray field expressed with vector potential

$$\mathbf{A}(\mathbf{r}, t) = \mathbf{A}_0 \exp(i\mathbf{k} \cdot \mathbf{r} - i\omega t) \ , \quad \mathbf{E} = -\frac{\partial \mathbf{A}}{\partial t} \ , \quad \mathbf{B} = \nabla \times \mathbf{A} \ .$$

Interaction with electron. Momentum increased by field term.

$$\mathbf{p} \longrightarrow \mathbf{p} - \frac{e}{c}\mathbf{A}(\mathbf{r}, t)$$

$$\frac{\mathbf{p}^2}{2m} \longrightarrow \frac{\mathbf{p}^2}{2m} - \frac{e}{mc}\mathbf{A}(\mathbf{r}, t) \cdot \mathbf{p} + \frac{e}{2mc}[\mathbf{p}, \mathbf{A}] + \frac{e^2}{2mc^2}\mathbf{A}^2$$

$$\frac{\mathbf{p}^2}{2m} \longrightarrow \frac{\mathbf{p}^2}{2m} - \frac{e}{mc}\mathbf{A}(\mathbf{r},t)\cdot\mathbf{p} + \frac{e}{2mc}[\mathbf{p},\mathbf{A}] + \frac{e^2}{2mc^2}\mathbf{A}^2$$

Coulomb gauge $\nabla \cdot \mathbf{A} = 0 \rightarrow [\mathbf{p},\mathbf{A}] = 0$.
$\mathbf{A}$ term $\rightarrow$ single photon processes = absorption, stimulated emission.
$\mathbf{A}^2$ term $\rightarrow$ two-photon processes (esp. scattering).

$\rightarrow$ Interaction Hamiltonian for absorption

$$H_{\rm int}(t) = H_{\rm int}\exp(-i\omega t)\ , \quad H_{\rm int} = -\frac{e}{mc}\sum_i \mathbf{A}(\mathbf{r}_i)\cdot\mathbf{p}_i$$

1st order perturbation $\rightarrow$ transition rate "Fermi's Golden Rule"

$$W_{if} = \frac{2\pi}{\hbar}|\langle\phi_f|H_{\rm int}|\phi_i\rangle|^2\delta(E_f - E_i - \hbar\omega)$$

($H(t) \sim \exp(i\omega t) \rightarrow$ $W_{if} \sim \delta(E_f - E_i + \hbar\omega) \rightarrow$ stimulated emission)

XAS formula

X-ray beam = plane wave with polarization $\mathbf{e}$. $\mathbf{A}_0(\mathbf{r}) = \mathbf{e}A_0 \exp(i\mathbf{k}\cdot\mathbf{r})$.

$h\nu < 1$ keV $\Leftrightarrow$ $\lambda > 12$ Å, much larger than core orbital.

$\Rightarrow$ for matrix element calculation, $\exp(i\mathbf{k}\cdot\mathbf{r}) \approx 1$ "dipole approximation"

Instead of $\mathbf{p}$, we can use $\mathbf{r}$. $[\mathbf{r}, H] = \frac{i\hbar}{m}\mathbf{p}$ and $|\phi\rangle$'s are eigenstates of H.

Then, dropping all constants, the XAS intensity for a given initial state Φ_{ini}

$$I_{\mathrm{ini}}(\omega) = \sum_f |\langle \Phi_f | \mathbf{e} \cdot \sum_i \mathbf{r}_i | \Phi_{\mathrm{ini}} \rangle|^2 \, \delta(E_f - E_{\mathrm{ini}} - \omega)$$

At low T, only ground state populated, so

$$I(\omega) = \sum_f |\langle \Phi_f | \mathbf{e} \cdot \sum_i \mathbf{r}_i | \Phi_g \rangle|^2 \, \delta(E_f - E_g - \omega)$$

From many-electron to single-electron formula

$$I(\omega) = \sum_f |\langle \Phi_f | \mathbf{e} \cdot \sum_i \mathbf{r}_i | \Phi_g \rangle|^2 \, \delta(E_f - E_g - \omega)$$

If $\quad |\Phi_g\rangle = |\Phi_0^c\rangle|\phi_c\rangle \qquad |\Phi_f\rangle = |\tilde{\Phi}_j^c\rangle|\phi_k\rangle \qquad \langle\phi_k|\phi_c\rangle = 0$

$S_j \equiv \langle\tilde{\Phi}_j^c|\Phi_0^c\rangle \quad E_g = E_0^c + \epsilon_c \quad E_f = \tilde{E}_j^c + \epsilon_k \quad \Delta_j \equiv \tilde{E}_j^c - E_0^c$

$$I(\omega) = \sum_j |S_j|^2 \sum_k |\langle \phi_k | \mathbf{e} \cdot \mathbf{r} | \phi_c \rangle|^2 \, \delta(\epsilon_k - \epsilon_c - \omega + \Delta_j)$$

$$= \sum_k |\langle \phi_k | \mathbf{e} \cdot \mathbf{r} | \phi_c \rangle|^2 \, \delta(\epsilon_k - \epsilon_c - \omega) \; * \; \sum_j |S_j|^2 \delta(\omega - \Delta_j)$$

Convolution of one-electron XAS formula with $N-1$ electron excitation spectrum ($\sim$ core-level XPS).

Single-electron approximation

Only $j = 0$ ("fully relaxed channel") $\rightarrow$

$$I(\omega) = |S_0|^2 \sum_k |\langle \phi_k | \mathbf{e} \cdot \mathbf{r} | \phi_c \rangle|^2 \, \delta(\epsilon_k - \tilde{\epsilon}_c - \omega) \, , \qquad \tilde{\epsilon}_c = \epsilon_c - \Delta_0$$

- XAS can be calculated approximately from single electron states ϕ_c and ϕ_k.
- Intensity reduced $|S_0| < 1$. Rest $1 - |S_0|$ in many-body excited states ($\sim$ photoemission shake-up satellites etc) which adds to background.
- Core-level energy shifted by $N - 1$ electron relaxation energy to core-hole, Δ_0. (In practice $\epsilon_k - \tilde{\epsilon}_c = E_f - E_g$, from ΔSCF calc.)

Core hole — orbital relaxation — screening

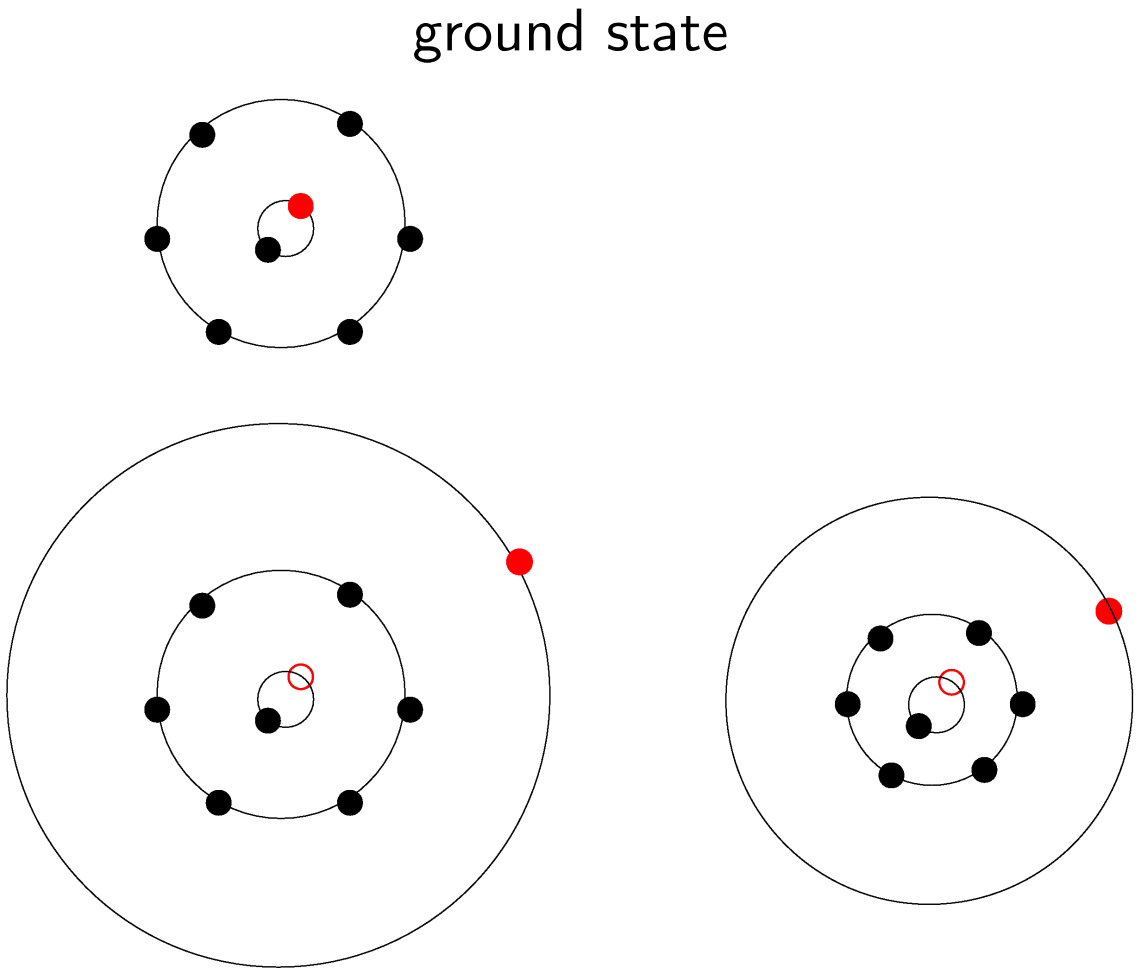

What is the best potential for final state $|k\rangle$?

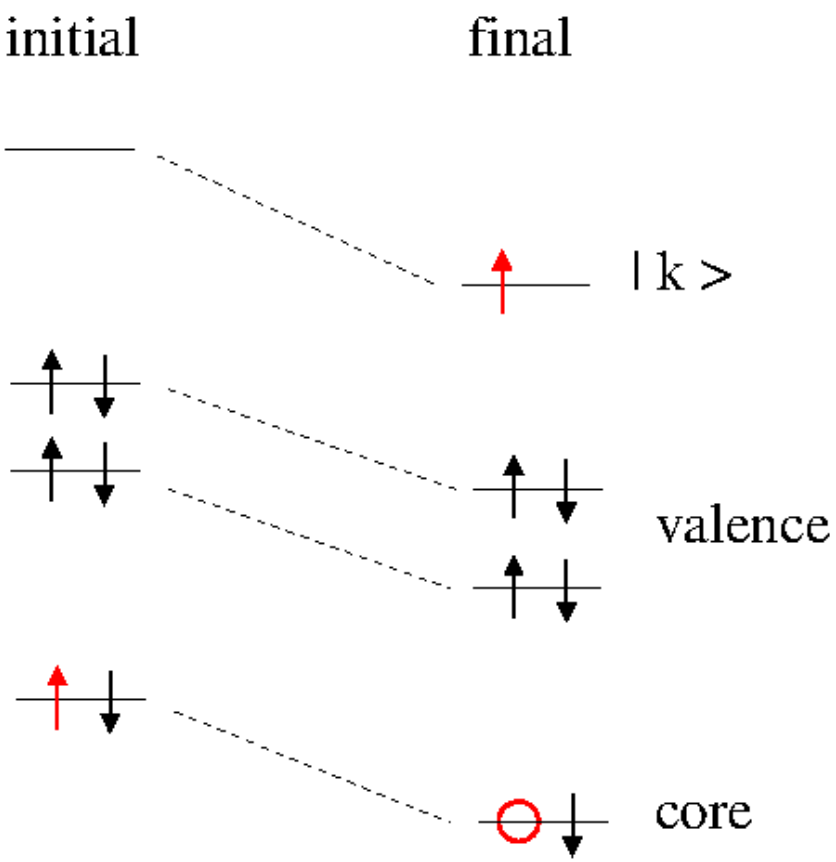

Final state rule

photoelectron wave function $|k\rangle$ computed in presence of core-hole, and all electronic states fully relaxed

Slater transition state

compute $|c\rangle$ and $|k\rangle$ with half a core-hole
transition: ground (0 holes) to final (1 hole)

in solids: impurity problem, supercell calculation

Dipole selection rules

Matrix element $\langle \phi_k | \mathbf{e} \cdot \mathbf{r} | \phi_c \rangle$. Expand ϕ_k in atomic-like orbitals at sites $\mathbf{R}_i$.

$$\phi_k = \sum_{ilm} B^k_{ilm} \phi_{ilm} \ , \quad \phi_{ilm}(\mathbf{r}) = R^k_{il}(r_i) Y_{lm}(\Omega_i) \ , \quad \mathbf{r}_i \equiv \mathbf{r} - \mathbf{R}_i \equiv (r_i, \Omega_i)$$

Y_{lm} are spherical harmonics = complete, orthonormal set of angular functions ($\sim$ s,p,d,f... orbitals). The core-orbital is localized at site i_c, so only orbitals at i_c contribute to the matrix element.
Consider core-s state and linearly polarized light along z, $\mathbf{e} = \mathbf{z}$.
$\mathbf{e} \cdot \mathbf{r} = z = r Y_{10} \sqrt{4\pi/3}$ spherical harmonic

$$\langle \phi_{lm} | z | \phi_s \rangle = \int d\Omega \, dr \, r^2 \ R_l \, Y^*_{lm} \ z \ R_s \, Y_{00} = \frac{1}{\sqrt{3}} \int dr \ r^3 R_l R_s \int d\Omega \, Y^*_{lm} Y_{10}$$

Y_{lm} orthonormal set $\Rightarrow$ only $(lm) = (10)$ gives non-zero integral.

$\Rightarrow$ selection rule $\quad \langle \phi_{lm} | z | \phi_s \rangle = 0$, except for $(lm) = p_z$.

Light polarization $q = 0$ linear z, $q = \pm 1$ circular left/right.
Wigner-Eckart theorem

$$\langle n' l' m' s' | r_q | n l m s \rangle = \delta_{s's} \, (-1)^{l'-m'} \begin{pmatrix} l' & 1 & l \\ -m' & q & m \end{pmatrix} \langle n' l' || r || n l \rangle$$

Wigner 3-j symbols $(\ldots)$ (=angular integrals) non-zero only for:

$$\boxed{l' = l \pm 1 \qquad m' = m + q \qquad s' = s}$$

dipole selection rules

circular pol., spherical harmonics

q	s	p_0	p_1	p_{-1}
0	p_0	s,d_0	d_1	d_{-1}
1	p_1	d_1	d_2	s, d_0
-1	p_{-1}	d_{-1}	s, d_0	d_{-2}

linear pol., cubic harmonics

q'	s	p_x	p_y	p_z
x	p_x	s, d_e	d_{xy}	d_{xz}
y	p_y	d_{xy}	s, d_e	d_{yz}
z	p_z	d_{xz}	d_{yz}	s, d_e

$d_e = \{d_{x^2-y^2}, d_{3z^2-r^2}\}$

Density of states (DOS)

Eigenstates ψ_k, eigenvalues ϵ_k.

$$\rho(\epsilon) = \sum_k \delta(\epsilon - \epsilon_k) \quad \text{total DOS}$$

$$\rho(\epsilon, \mathbf{r}) = \sum_k |\psi_k(\mathbf{r})|^2 \delta(\epsilon - \epsilon_k) \quad \text{local (point) DOS}$$

$$\rho_{ilm}(\epsilon) = \sum_k |\langle \phi_{ilm} | \psi_k \rangle|^2 \delta(\epsilon - \epsilon_k) \quad \text{partial (ilm) DOS}$$

ϕ_{ilm} = normalized basis function centered on site i, symmetry lm

XAS and DOS

$$I_q(\omega) = \sum_k |\langle \psi_k | r_q | \phi_c \rangle|^2 \, \delta(\epsilon_k - \epsilon_c - \omega)$$

Develop $|k\rangle$ in local basis $|ilm\rangle$

$$\langle k | r_q | i_c l_c m_c \rangle = \sum_{ilm} \langle k | ilm \rangle \langle ilm | r_q | i_c l_c m_c \rangle$$

$$= \sum_{\pm} \langle k | i_c, l_c \pm 1, m + q \rangle \langle i_c, l_c \pm 1, m + q | r_q | i_c l_c m_c \rangle$$

Localization of $|c\rangle$ and selection rules $\rightarrow$ only one or two terms survive, e.g. $c = s$, $q = z \Rightarrow \langle || \rangle = 0$ except for $i = 0$, $(lm) = p_0$

$$I_q(\omega) = \sum_{\pm} \sum_k |\langle k | i_c l_{\pm} m \rangle \langle i_c l_{\pm} m | r_q | c \rangle|^2 \, \delta(\epsilon_k - \epsilon_c - \omega)$$

$$I_q(\omega) \approx \sum_{\pm} |\langle i_c l_\pm m | r_q | c \rangle|^2 \sum_k |\langle k | i_c l_\pm m \rangle|^2 \, \delta(\epsilon_k - \epsilon_c - \omega)$$

$$I_q(\omega) \;\sim\; A_+ \rho_{i_c l_+ m}(\omega + \epsilon_c) + A_- \rho_{i_c l_- m}(\omega + \epsilon_c)$$

K-edge, $s \to p$, $A_- = 0$. $L23$ edges often $A_+ \gg A_-$
So, in single electron approximation, the

XAS is approximately proportional to a partial DOS at absorber site

Example: K-edge, x-polarization. XAS $\sim$ p_x-DOS

$\to$ **element-resolved / local electronic structure** (unoccupied states)

Example: SrTiO3, O-K edge

Partial density of states from DFT (Wien2k) code

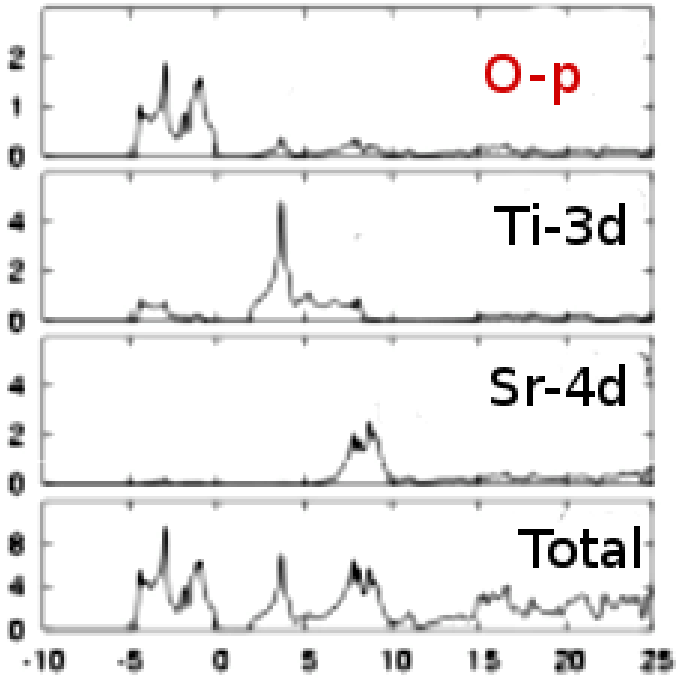

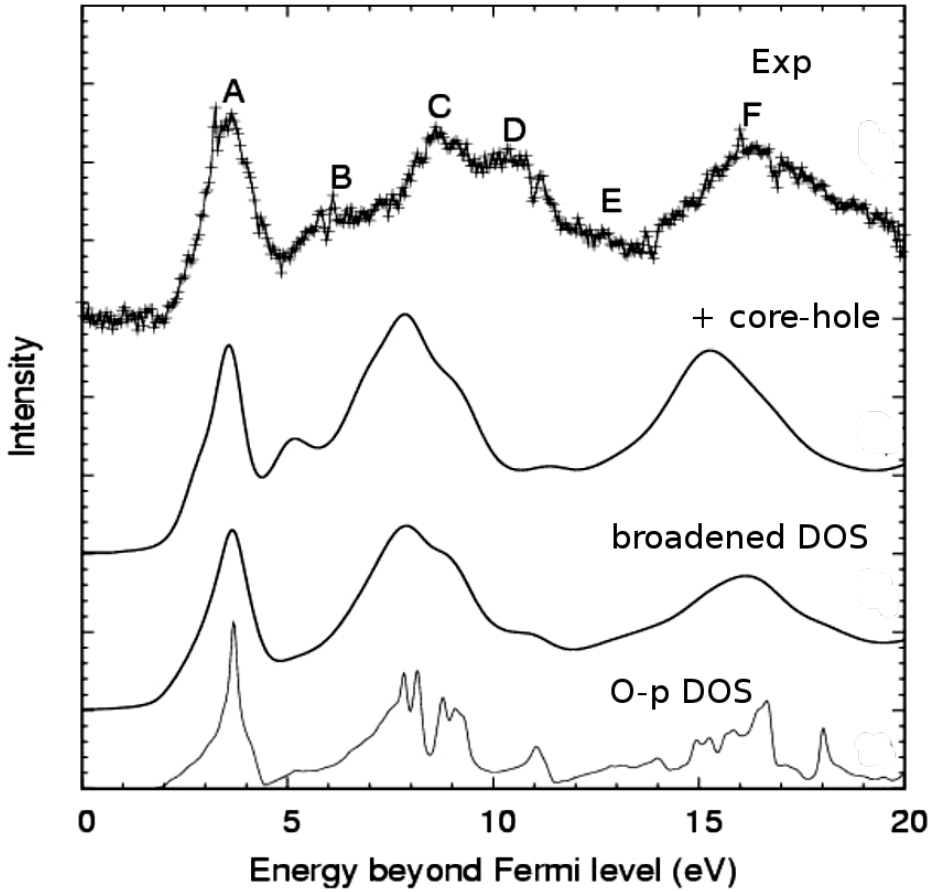

XAS spectrum essentially broadened O-p projected DOS. Some improvement with final state rule.
[G. Ratdke, G. Botton, Microscopy and Microanalysis 2010]

Multiple scattering

Continuum wave expanded in energy-dependent spherical waves $|ilm\rangle$ located at sites i.

$$|\mathbf{k}\rangle = \sum_{ilm} B^{\mathbf{k}}_{ilm} |ilm\rangle$$

$$B^{\mathbf{k}}_{ilm} = \sum_{jl'm'} \tau_{ilm,jl'm'} A^{\mathbf{k}}_{jl'm'}$$

$A^{\mathbf{k}}_{jl'm'}$ = plane-wave coefficients
τ_{ij} = scattering path operator

$$\tau_{ij} = \delta_{ij} t_i + t_i G_{ij} t_j + t_i \sum_k G_{ik} t_k G_{kj} t_j + \ldots$$

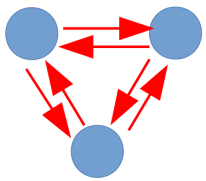

t_i atomic scattering matrix (phase shifts)
G_{ij} free electron propagator

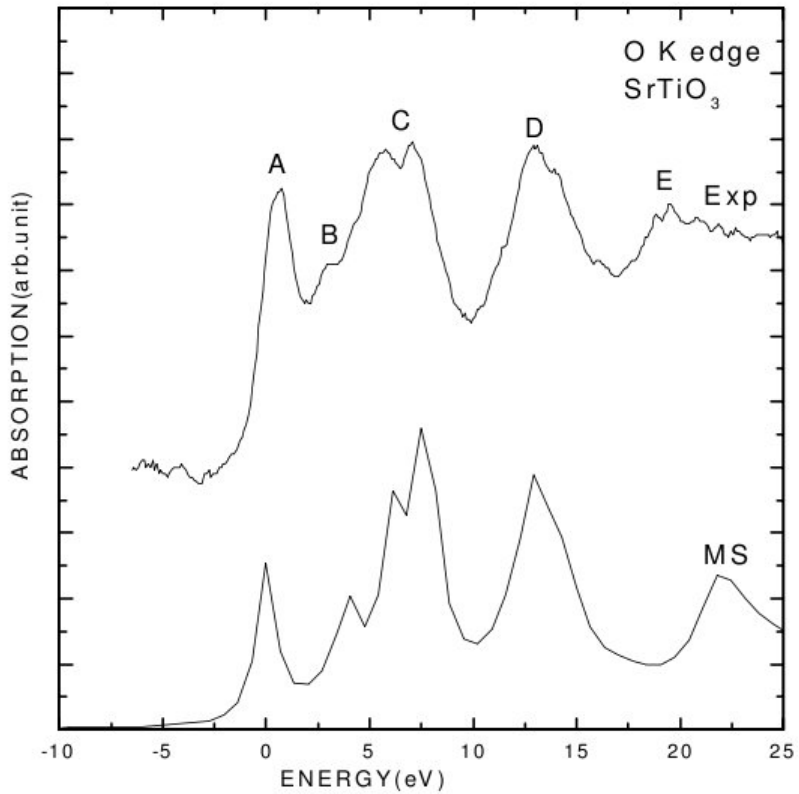

Z. Wu et al J. Synchrotron Rad. (2001)

Dichroism

= polarisation dependence of light absorption

Linear Dichroism (LD) is the difference in absorption of light linearly polarized parallel and perpendicular to an orientation axis (e.g. molecular axis, crystal axis, magnetisation direction)

$$\mathrm{LD} = I(\parallel) - I(\perp) = I_z - I_x$$

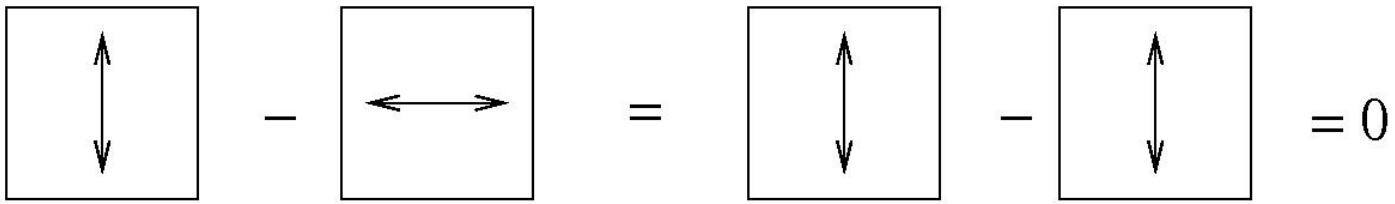

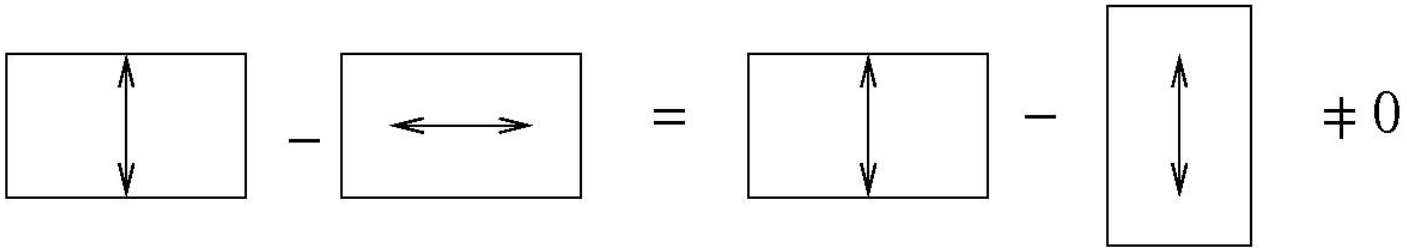

LD is sensitive to anisotropy of electronic density (and/or atomic structure) around the absorber site

Linear dichroism

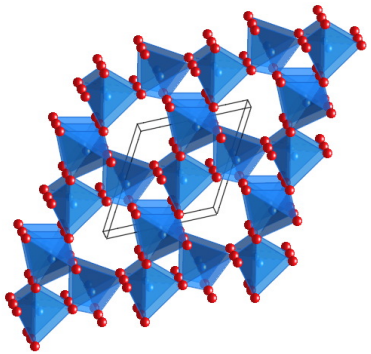

α-quartz single crystal

hexagonal, c$\neq$a $\Rightarrow$ LD$\neq$ 0
$I(||) - I(\perp) \sim \rho_{pz} - \rho_{px}$

Si K-edge XAS
[Taillefumier et al. PRB 2002]

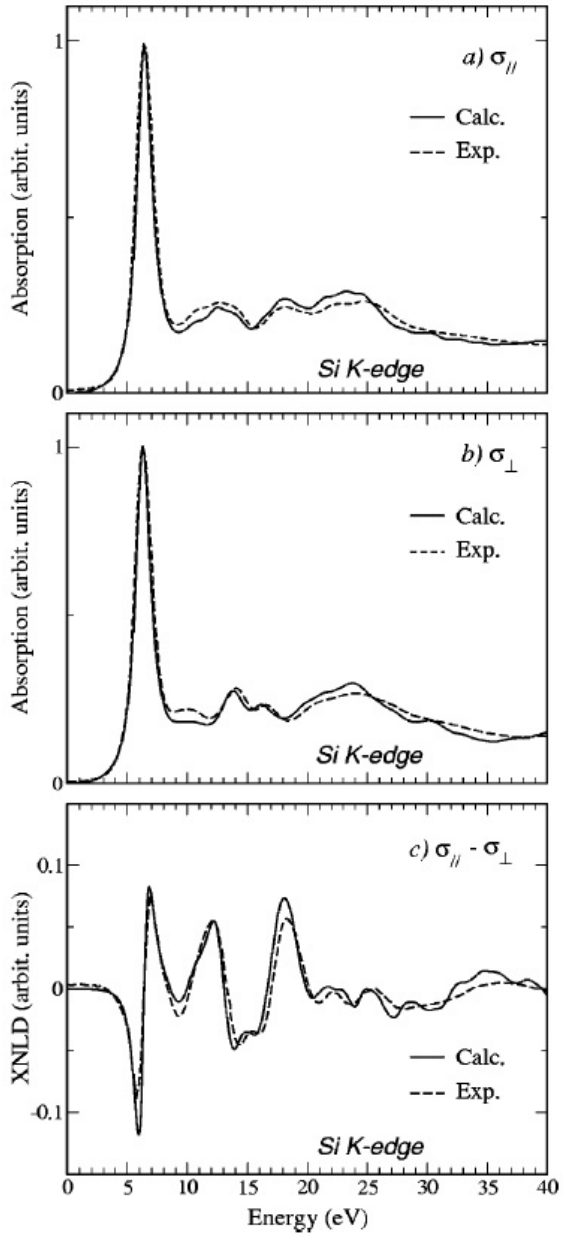

FIG. 2. Experiumental (dashed line) and calculated (solid line) Si *K*-edge polarized x-ray absorption spectra in α-quartz: (a) $\sigma_{\|}$ corresponding to $\varepsilon \| [001]$; (b) $\sigma_{\perp}$ corresponding to $\varepsilon \perp [001]$; (c) XNLD or $\sigma_{\|}$-$\sigma_{\perp}$. A 1840.7 eV shift was applied to experimental data.

Circular Dichroism

is the difference in absorption of left- and right-handed circularly polarized light.

Right circularly polarized light

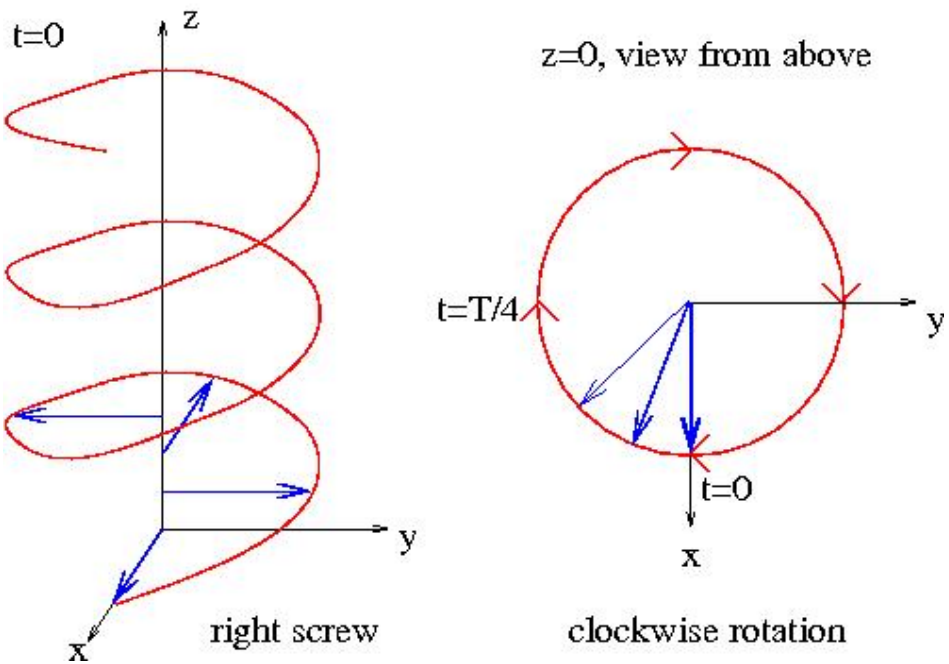

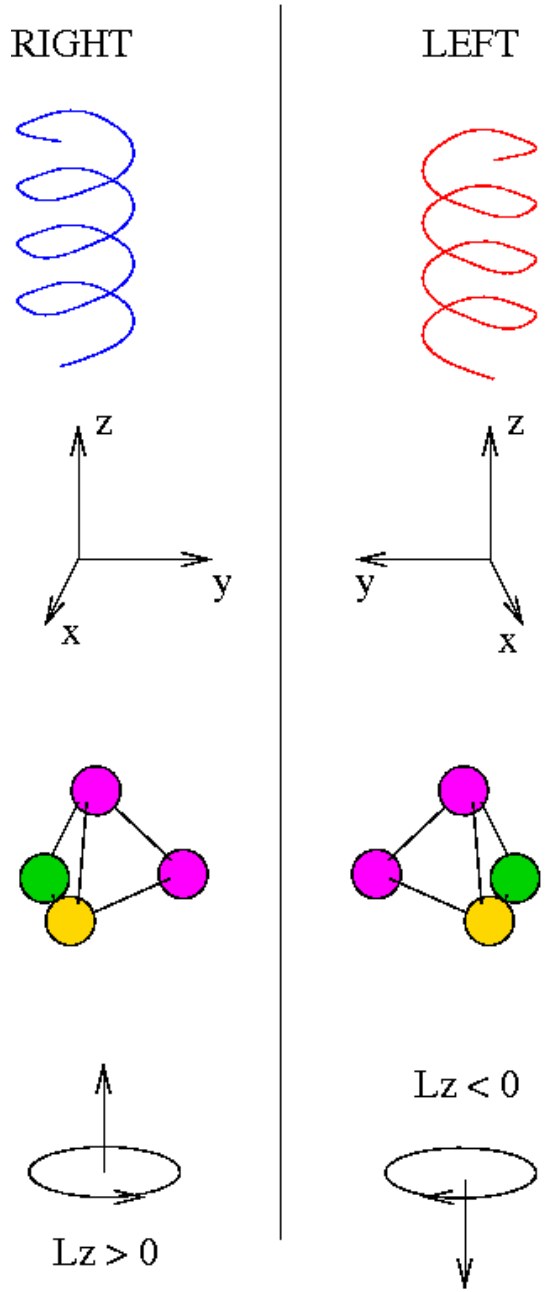

Chirality/Handedness

X-ray circular dichroism of chiral molecules

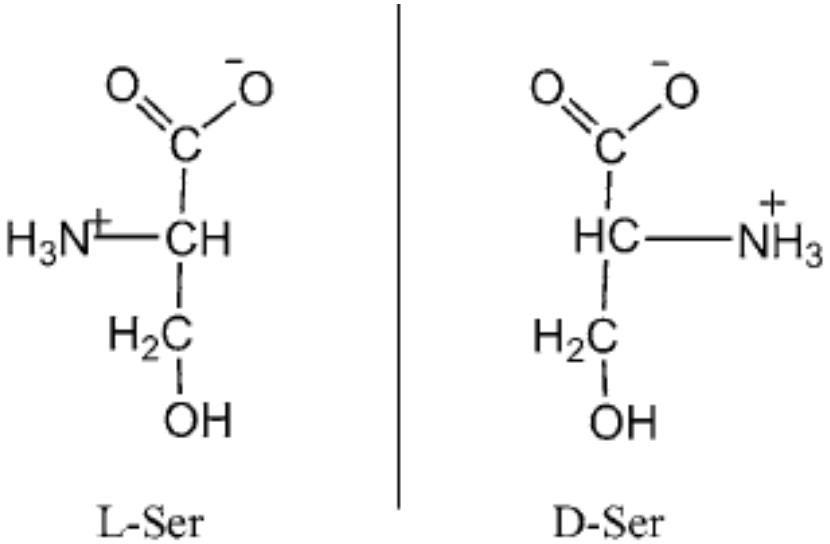

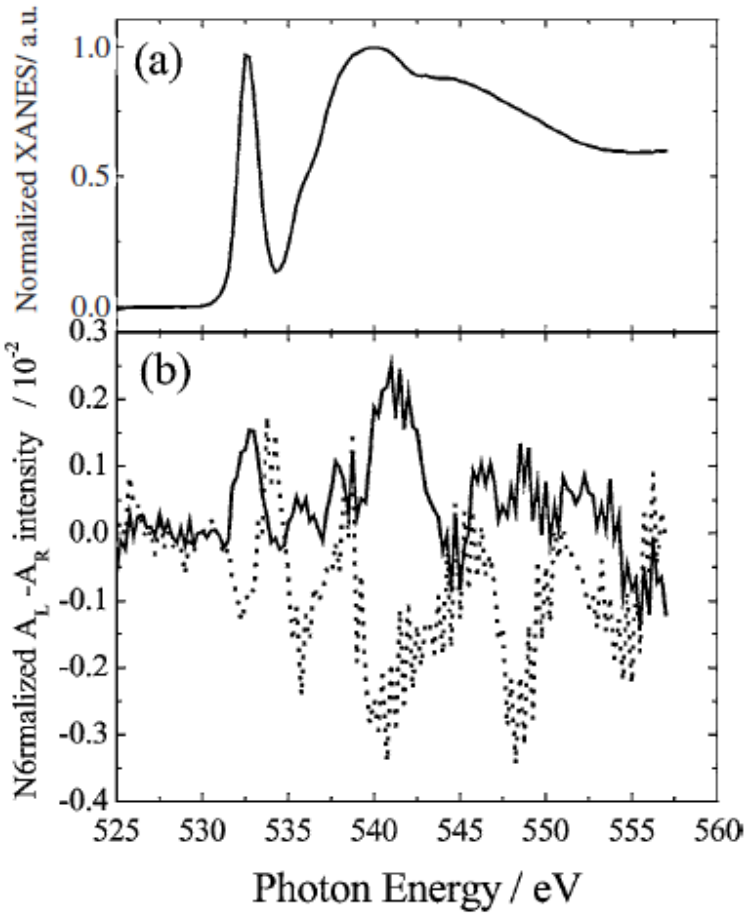

Serine. [Physica Scripta T115, 873]

$\sim$ optical activity. But effect much weaker for x-rays than vis-UV light.

X-ray Magnetic Circular Dichroism

VOLUME 58, NUMBER 7 PHYSICAL REVIEW LETTERS 16 FEBRUARY 1987

Absorption of Circularly Polarized X Rays in Iron

G. Schütz, W. Wagner, W. Wilhelm, and P. Kienle[a]
Physik Department, Technische Universität München, D-8046 Garching, West Germany

R. Zeller
Institut für Festkörperforschung der Kernforschungsanlage Jülich, D-5175 Jülich, West Germany

and

R. Frahm and G. Materlik
Hamburger Synchrotronstrahlungslabor am Deutsches Elektronen-Synchrotron DESY, D-2000 Hamburg 52, West Germany
(Received 22 September 1986)

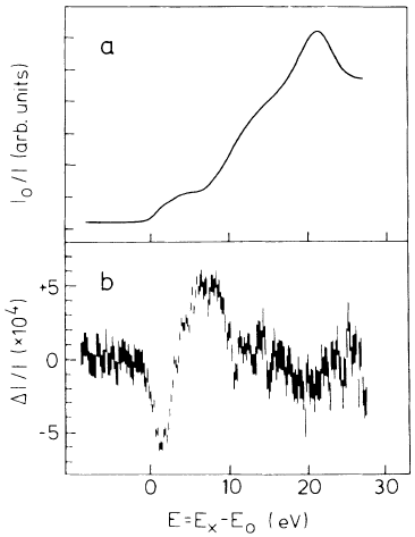

FIG. 1. (a) Absorption I_0/I of x rays as function of the energy E above the K edge of iron and (b) the difference of the transmission $\Delta I/I$ of x rays circularly polarized in and opposite to the direction of the spin of the magnetized d electrons.

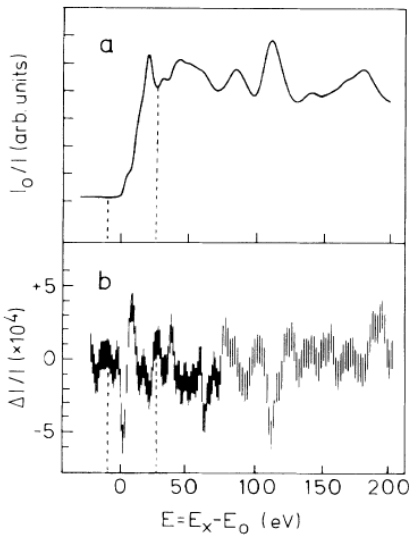

FIG. 2. (a) Extended x-ray absorption fine structure of iron in the energy region up to 200 eV above E_0 and (b) the spin-dependent transmission $\Delta I/I$. The energy region marked by dashed lines corresponds to the energy region shown in Fig. 1.

Fe K-edge.

Origin of magnetic circular dichroism

circular light is chiral (= parity-odd) but also **time-reversal odd** $\longrightarrow$ dichroism for time-reversal broken states

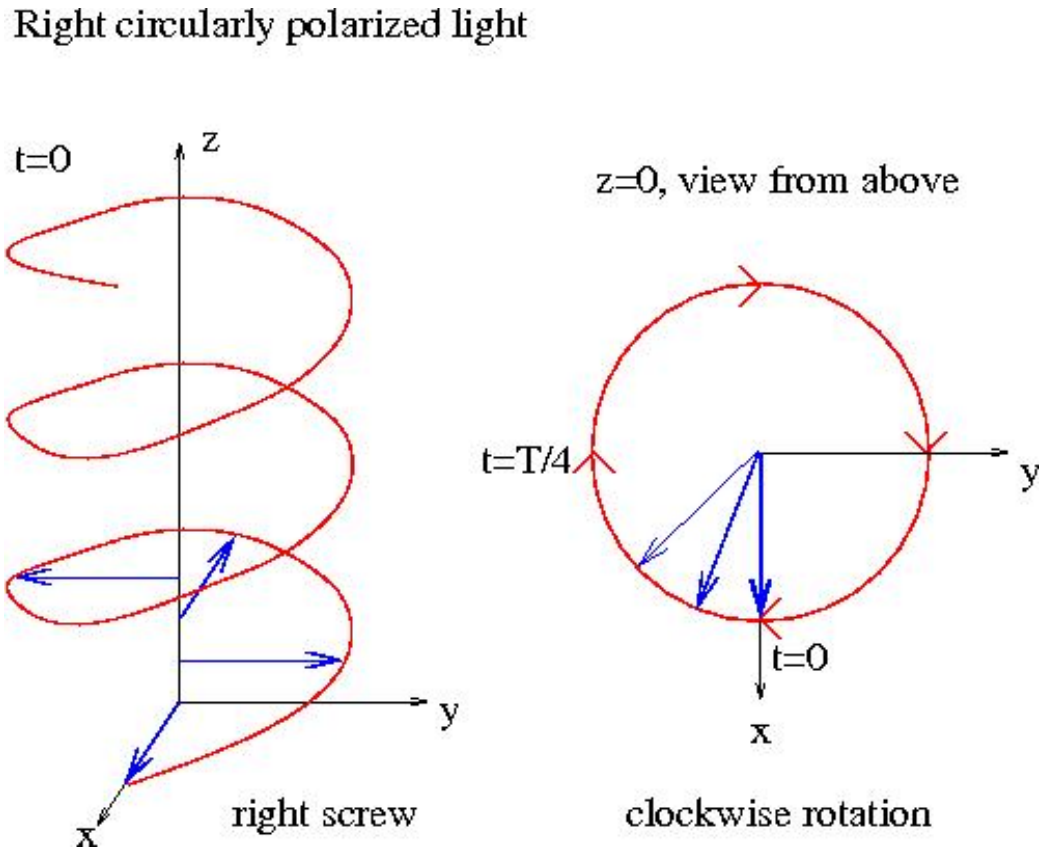

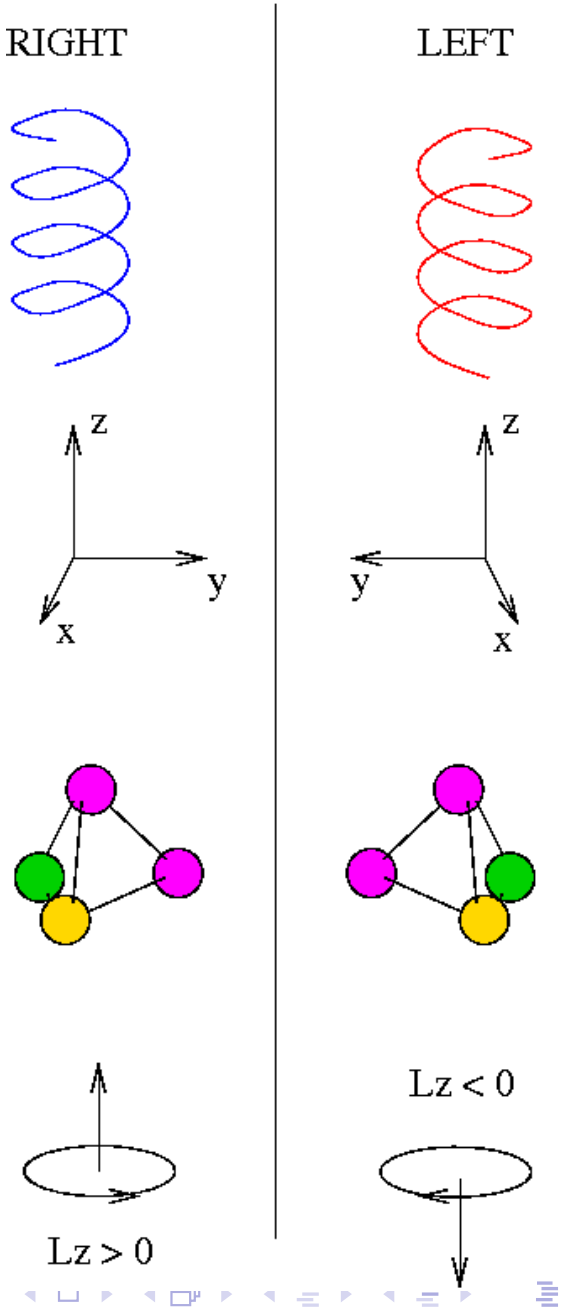

Circular light has angular momentum (helicity)

absorption $\rightarrow$ angular momentum transferred to orbital moment of electron

if states orbitally polarized $\rightarrow$ transition probabilites different for left/right

$\rightarrow$ circular dichroism detects orbital polarization of electronic states

Ex. K-edge. $1s \rightarrow p$.

XMCD $\sim$ DOS(p_+) - DOS(p_-)

orbital magnetic polarization $L_z(\epsilon)$ of p-projected conduction band

However, orbital polarization of conduction-p band usually small, because spin-orbit coupling $\ll$ hybridization

L23-edge ($2p \rightarrow 3d$) XMCD of transition elements

Strong absorption "white lines". Strong XMCD.

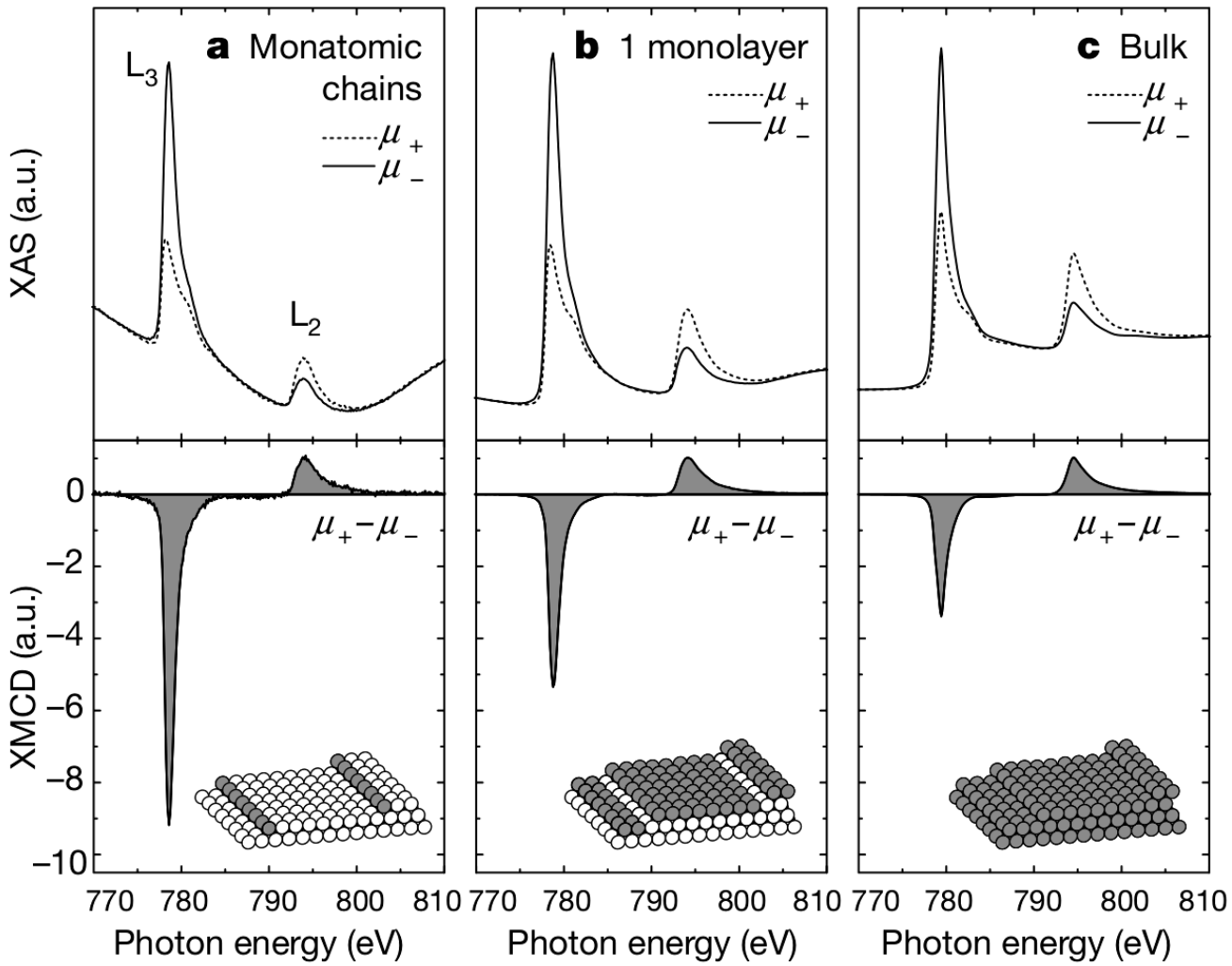

Co / stepped Pt(111)

wire, ML, bulk

strong variation of Co orbital magnetic moment [μ_B]

wire	ML	bulk
0.68	0.37	0.31

obtained with "XMCD sum rules"

P. Gambardella et al. Nature 416, 301 (2001)

L23-edge XMCD

$$I_q(m) = \sum_{m_c} |\langle dm|r_q|m_c\rangle|^2$$

$$= R_{dp}^2 A_q(m)$$

m	A_-	A_0	A_+	XMCD $A_+ - A_-$	XAS $\sum_q A_q$
-2	6			-6	6
-1	3	3		-3	6
0	1	4	1	0	6
1		3	3	3	6
2			6	6	6

$$\text{XAS} = \sum_{mq} I_q(m)\langle \bar{n}_m\rangle = 6\, R_{dp}^2\, \langle n_h\rangle$$

$\langle \bar{n}_m\rangle = \#$ holes in orbital (dm), $\langle n_h\rangle = \#$ holes in 3d shell.

$$\text{XMCD} = \sum_m (I_+(m) - I_-(m))\langle \bar{n}_m\rangle = R_{dp}^2 \sum_m 3m\, \langle \bar{n}_m\rangle = -3\, R_{dp}^2\, \langle l_z\rangle$$

$$\frac{\text{XMCD}}{\text{XAS}} = -\frac{\langle L_z\rangle}{2\langle n_h\rangle}$$ orbital sum rule [B.T.Thole et al. PRL 1992]

Spin-orbit coupled p-states: $|j\mu\rangle = \sum_{m_c\sigma_c}(1\tfrac{1}{2}m_c\sigma_c|j\mu) \times |m_c\sigma_c\rangle$

$|\langle dm\sigma|r_q|j\mu\rangle|^2 = R^2_{dp}A_q(m,\sigma,j,\mu)$

A_q	$(\frac{3}{2},-\frac{3}{2})$	$(\frac{3}{2},-\frac{1}{2})$	$(\frac{3}{2},\frac{1}{2})$	$(\frac{3}{2},\frac{3}{2})$	$(\frac{1}{2},-\frac{1}{2})$	$(\frac{1}{2},\frac{1}{2})$
$-2\downarrow$	18_-					
$-1\downarrow$	9_0	6_-			3_-	
$0\downarrow$	3_+	8_0	1_-		4_0	2_-
$1\downarrow$		6_+	3_0		3_+	6_0
$2\downarrow$			6_+			12_+

Rel. transition probabilities to $d\downarrow$

	I_+	I_-	diff	sum
$2p3/2$	15	25	-10	40
$2p1/2$	15	5	10	20

Applies directly to $|g\rangle = |d^5,^6\,S\rangle$

$d\uparrow$ shell full, $d\downarrow$ shell empty.

E.g. high spin Mn^{2+}, Fe^3.

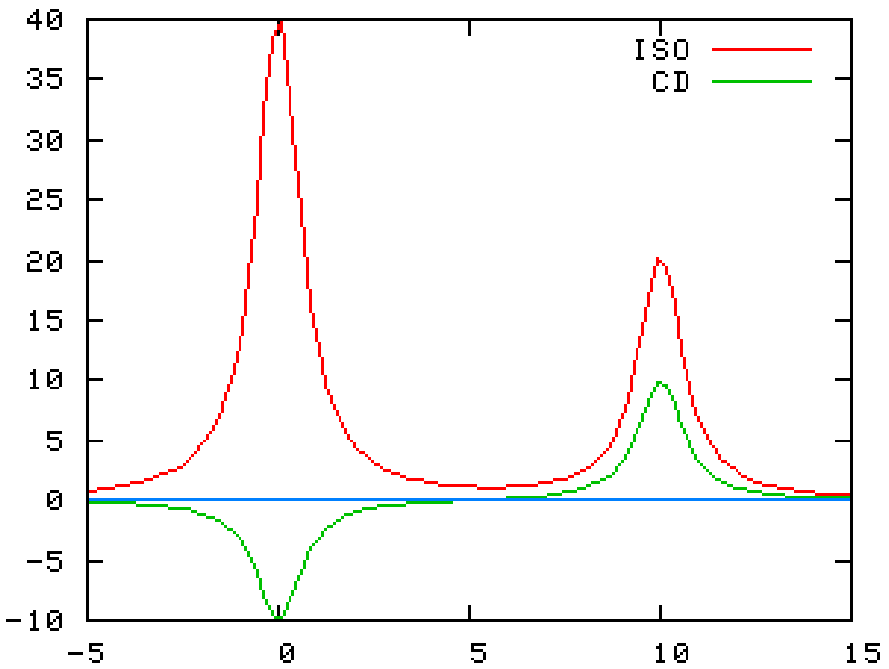

XMCD sum rules (for L23-edges)

[B. T. Thole et al. PRL 68, 1943 (1992). P. Carra et al. PRL 70, 694 (1993)]

If final 3d-orbital sufficiently localized then the (3d-) orbital moment of the atom can be found from integrated spectra as

$$\frac{\int_{L3+L2} XMCD}{\int_{L3+L2} XAS} = -\frac{\langle L_z \rangle}{2\langle n_h \rangle}$$

$\mathrm{XMCD} = I_+ - I_-, \quad \mathrm{XAS} = I_+ + I_- + I_0$
If $2p_{3/2} \rightarrow 3d$ and $2p_{1/2} \rightarrow 3d$ transitions do not mix, then also

$$\frac{\int_{L3} XMCD - 2\int_{L2} XMCD}{\int_{L3+L2} XAS} = -\frac{2\langle S_z \rangle + 7\langle T_z \rangle}{3\langle n_h \rangle}$$

T_z = magnetic dipole term.
Measures anisotropy of spin-density. Often negligible.

Sum rules have many limitations, but are easy to apply and very popular.

Correlation effects – many-electron theory

For transition metal (TM) $L23$-edges and rare-earths (RE) $M45$-edge the single electron formula for XAS yields very poor results.

Reason: spin and orbital degrees of freedom of core-hole strongly couple to the rather localized electrons in open final shell (3d in TM, 4f in RE)

This gives rise to strong configuration mixing between several Slater determinants, and thus the assumption $|\Phi_f\rangle = |\tilde{\Phi}^c_j\rangle|\phi_k\rangle$ is very bad.

Back to multielectron formula:

$$I(\omega) = \sum_f |\langle \Phi_f | \mathbf{e} \cdot \sum_i \mathbf{r}_i | \Phi_g \rangle|^2 \, \delta(E_f - E_g - \omega)$$

Multiplets

Multiplet is a term from atomic physics. For the same electronic configuration, i.e. C ($1s^2 2s^2 2p^2$) the energy levels of the many electron states split into multiplets (singlets, doublets, triplets,...).

The splting is due to the electron-electron Coulomb (and exchange) interaction.

For free atoms, total angular momentum $J = L + S$ is a good quantum number

when spin-orbit interaction is neglected (ok for light elements) then L and S are also individually good quantum numbers.

Ex. ($1s^2 2s^2 2p^2$) has three LS-terms:

$L = 2, S = 0$ (^1D), $L = 1, S = 1$ (^3P), $L = 0, S = 0$ (^1D).

The states of each term are degenerate, but there is energy splitting between the three terms.

Toy model for multiplet effects in XAS

$1s \rightarrow 2p$ absorption of a $(1s^2)$ or $(1s^2 2s^2)$ ground state

single-electron states
(= orbitals)

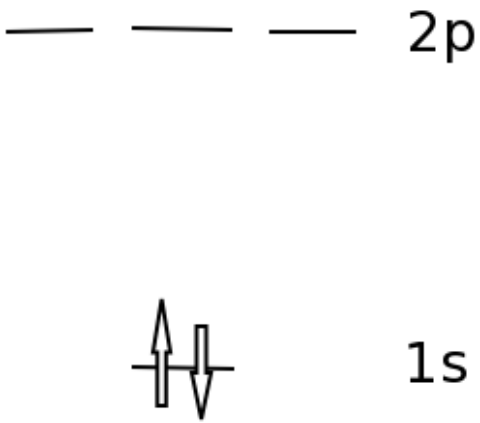

many-electron states

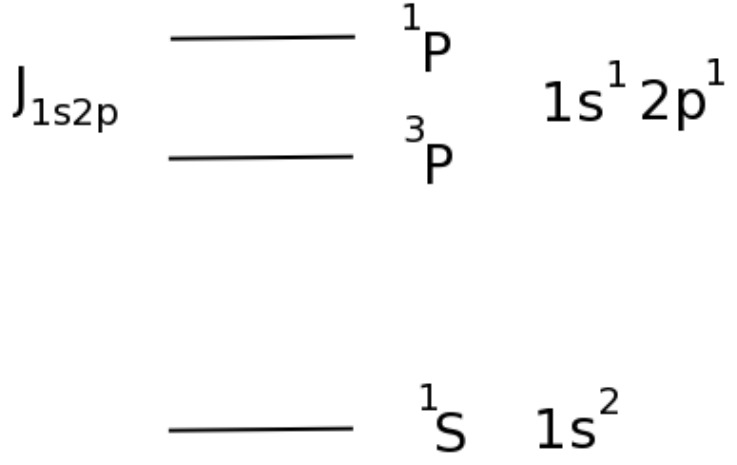

with spin-orbit coupling

single-electron states

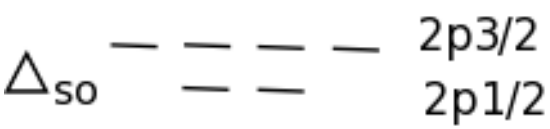

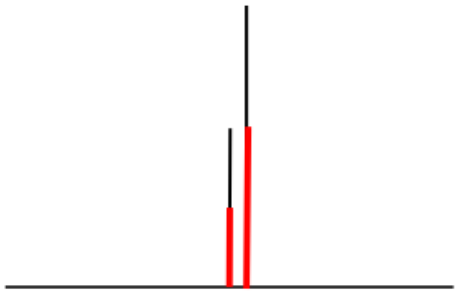

many-electron states

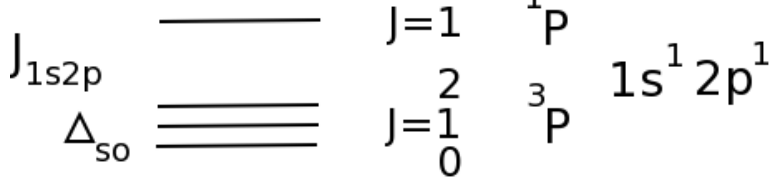

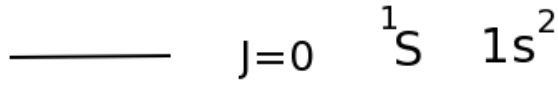

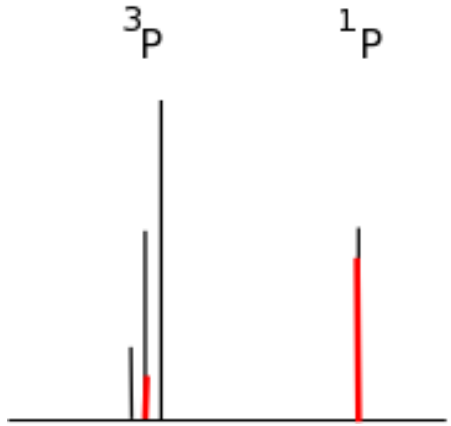

final levels and absorption intensities

L23- and M45-edge spectra: Crystal Field Multiplet model

Most popular method for calculating transition metal L23- and rare-earth M45-edge spectra based on:

R. Cowan: *Atomic structure and spectra* (1980) book + program
B.T. Thole adds crystal field and magnetism ($\sim$ 1985)
F.M.F. de Groot (Utrecht, NL) maintains code "CTM4XAS"

Choose element and valency, e.g. Mn4+
Ground state electronic conf.: $(1s^2 2s^2 2p^6 3s^2 3p^6 3d^3) = [\mathrm{Ar}]\ 3d^3$

Possible states: 3 electrons in 10 spin-orbs, $\begin{pmatrix} 10 \\ 3 \end{pmatrix} = 120$ states

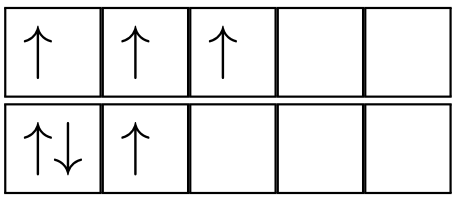

S=3/2, L=2+1+0=3 term ^4F

S=1/2, L=2+2+1=5 term ^2H

Form all possible basis states (Slater determinants) $|n\rangle$

Compute Hamiltonian matrix: $\langle n|H|m\rangle$

H = kinetic energy + V(electron-nuclei) + V(el.-el.) + spin-orbit
Matrix elements computed by Cowan's program for free ion

Diagonalize matrix $\langle n|H|m\rangle$

$\rightarrow$ energy levels (eigenvalues) and wave functions (eigenstates)
Eigenstates = linear combinations of Slater determinants (= basis states):
configuration interaction

Compute and diagonalize $\langle n|H|m\rangle$
Final state energy levels E_f and wavefunctions $|f\rangle$.
XAS $\sim |\langle f|\mathbf{e}\cdot\mathbf{r}|g\rangle|^2\delta(E_f - E_g - \omega)$

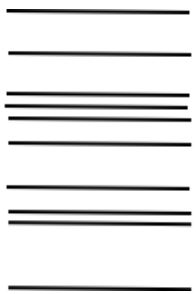

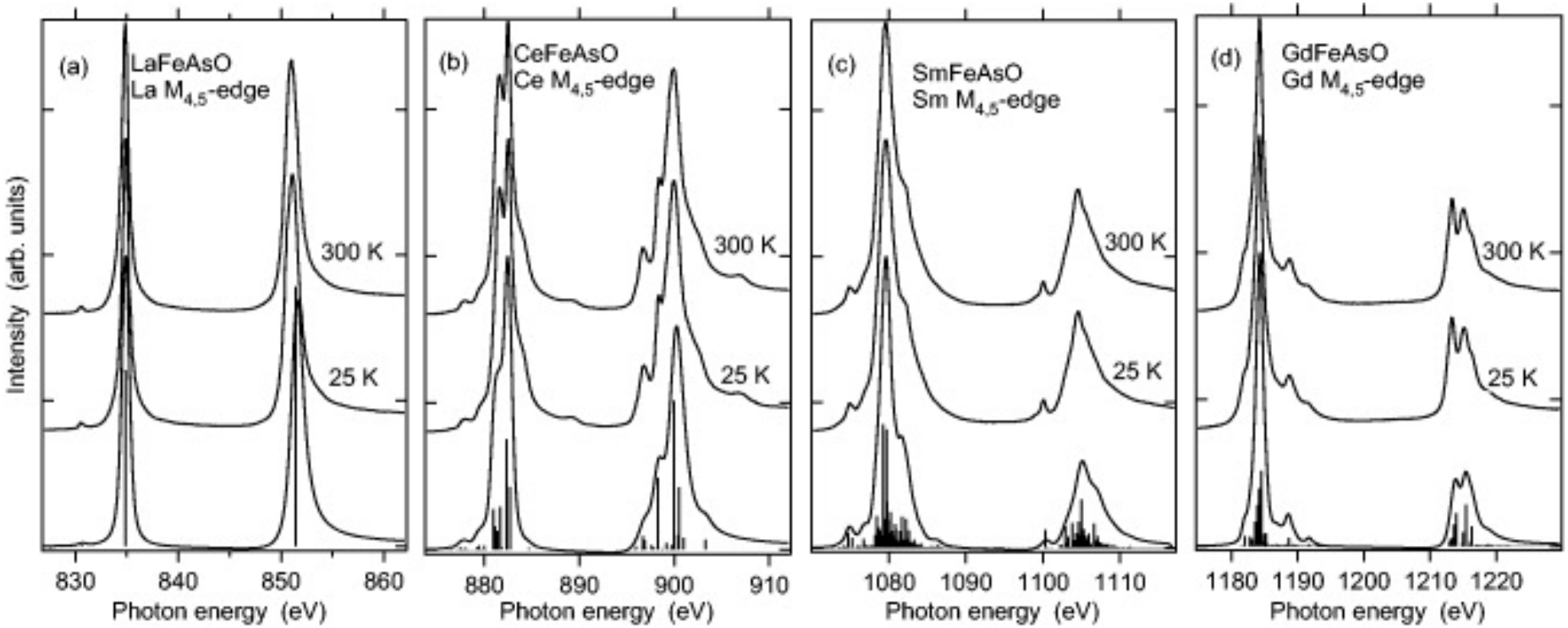

Rare-earth M45-edge (3d) absorption spectra.
Experiment and multiplet calculations (free ions. Cowan's program.)

[T. Kroll et al. New Journal Phys. 11 (2009) 025019.]

Solid ? Add **crystal field** according to point group of ion

Free ion: spherical

3d-level

Ion in cubic crystal field

Eg: z^2 x^2-y^2

Δ

T2g: xy yz zx

3d-derived levels in cubic crystal field

L23-edge spectrum

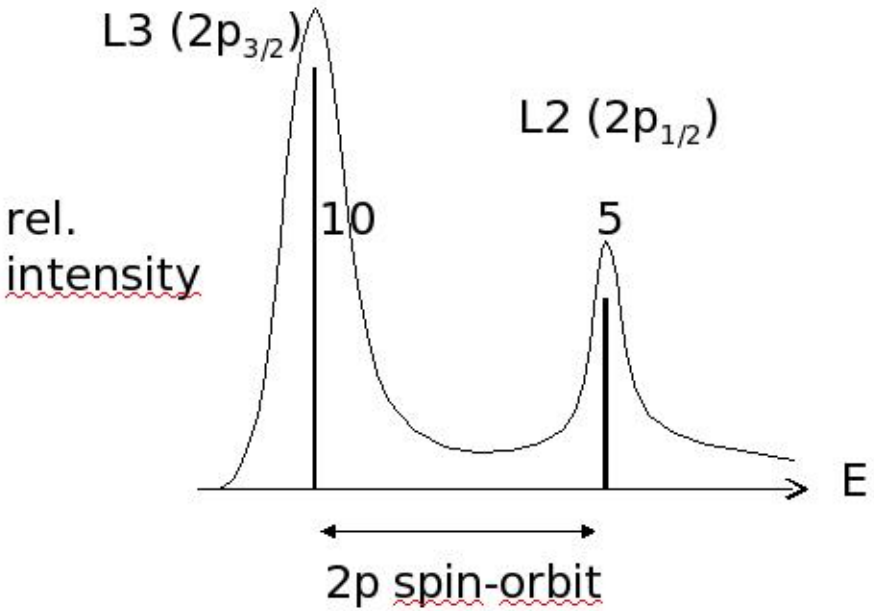

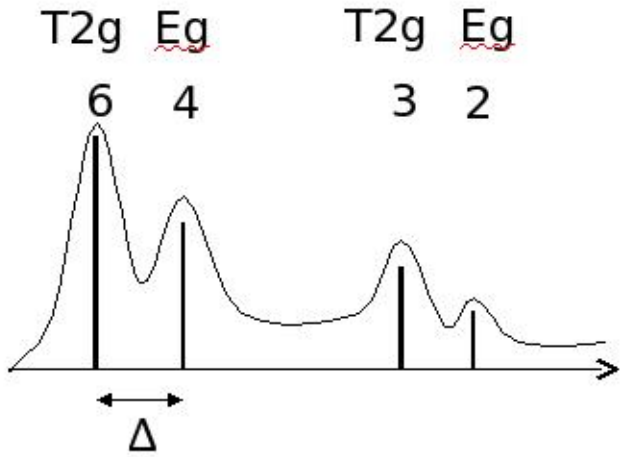

diagonalize H = H(atomic) + V(crystal field)

Multiplet interactions (coulomb, exchange integrals, spin-orbit) and crystal field comparable

$\rightarrow$ lots of lines, states all mixed up (L,S, spin-orbit, C.F.) simple assignment generally impossible

Crystal field approach very successful for ionic compounds in cubic symmetry (only one empirical CF parameter)

Covalent or metallic bonding, low symmetry $\rightarrow$
many CF parameters/reduction factors, CFM model questionable

Recently, several ab initio multiplet approaches.

- quantum chemistry "CAS-SCF" [H Ikeno et al PRB 83, 155107]
- Wannier-orbital approach [M. Haverkort et al PRB 85, 165113]
- particle-hole theories:
  - Time-dependent DFT [J. Schwitalla et al PRL 80, 4586]
  - Bethe-Salpeter equation [R Laskowski et al PRB 82, 205104]
  - Multichannel multiplet scattering [P. Krüger et al PRB 70, 245120]

X-ray absorption of individual titania nanostructures - Theory and STXM experiments

Peter Krüger　千葉　大学院融合科学　ナノ物性

Xiaohui Zhu

Adam Hitchcock

McMasters, Hamilton, Canada

Carla Bittencourt

University of Mons, Belgium

Why ?

- Titanium oxide has wide range of applications:
  catalysis, solar cells, paint, tooth paste …
- nanostructures enhance surface/bulk ratio → higher efficiency
- 1-D like shapes (nano-tubes, ribbons) promising for devices

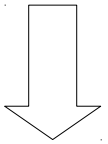

- prope and understand electronic structure of individual nanoparticles
- our tool: x-ray absorption spectroscopy + microscopy (STXM)

Scanning Transmission X-ray Microscopy

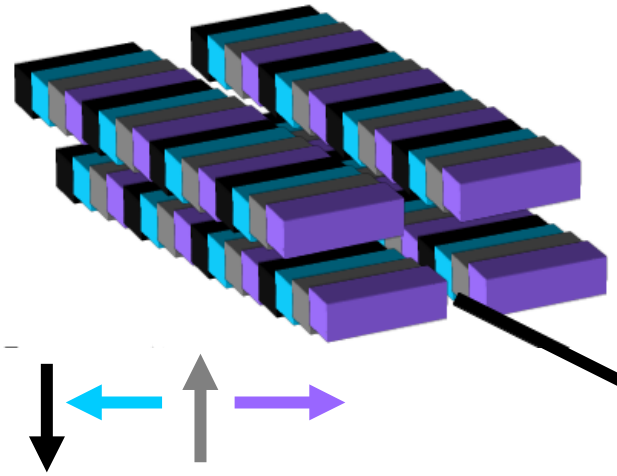

Canadian Light Source
SpectroMicroscopy Beamline

Elliptical Polarized Undulator
all 4 quadrants movable

Linear polarization any angle

Circular polarization

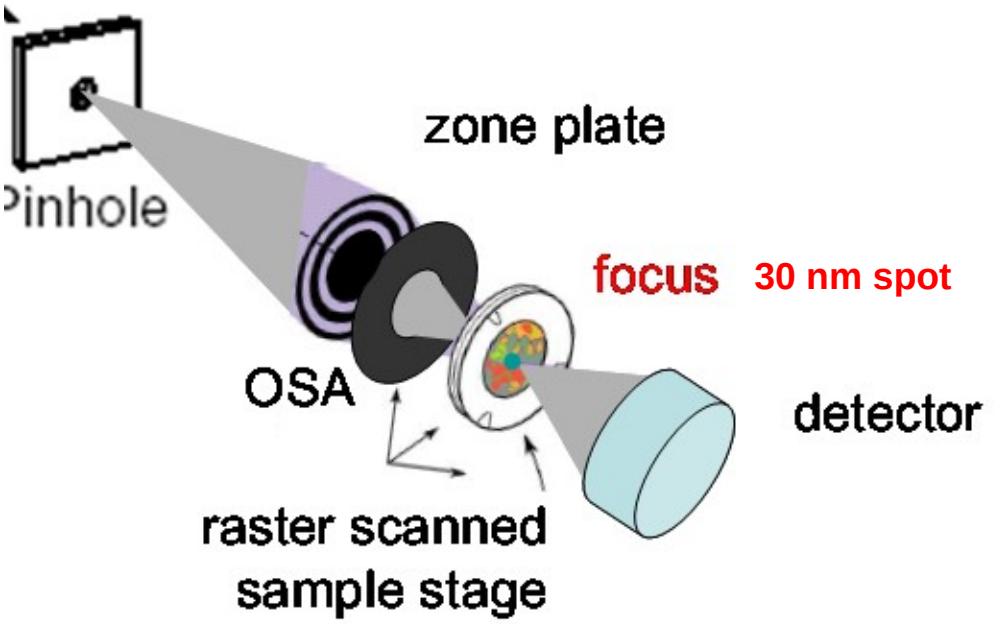

Na,H-Titanate nanotubes / “scrolls”

TiO_2 (anatase) + NaOH(aq) → $Na_xH_{2-x}Ti_3O_7$

hydrothermal synthesis T~ 95 - 135 C

[P. Umek et al., *J. Nanosci. Nanotechnol.* 7, 3502 (2007)]

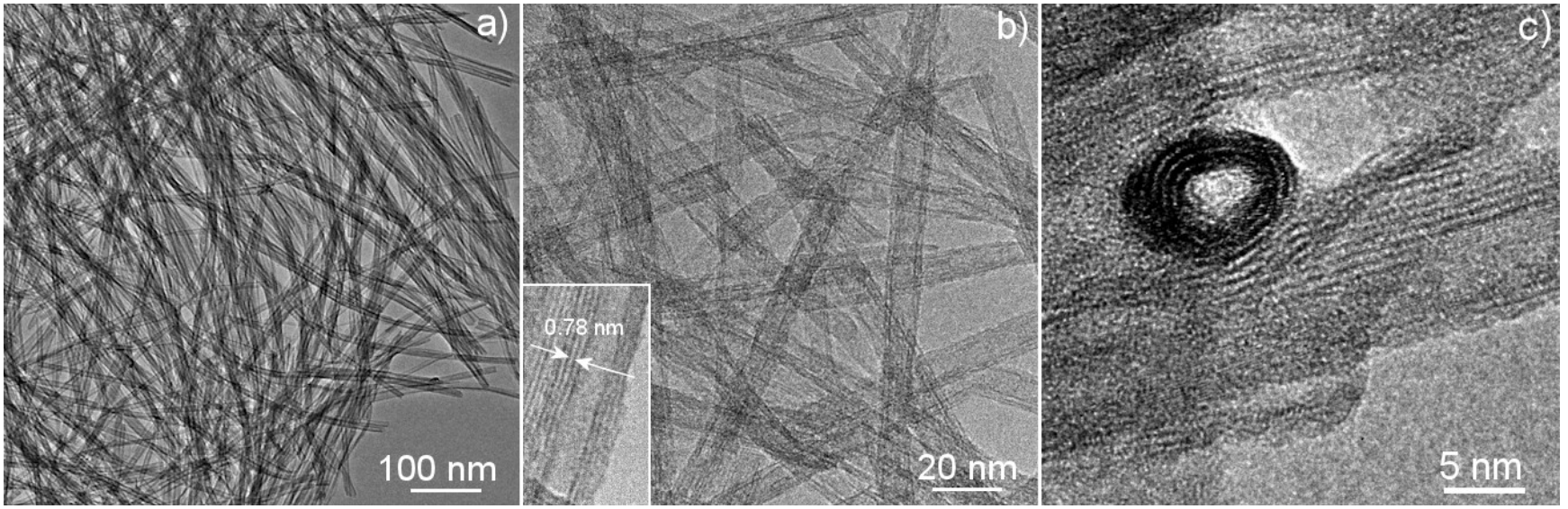

TEM

[C. Bittencourt, P. Krüger et al, B. J. Nanotechnol.3, 789 (2012)]

Structure of nanotubes

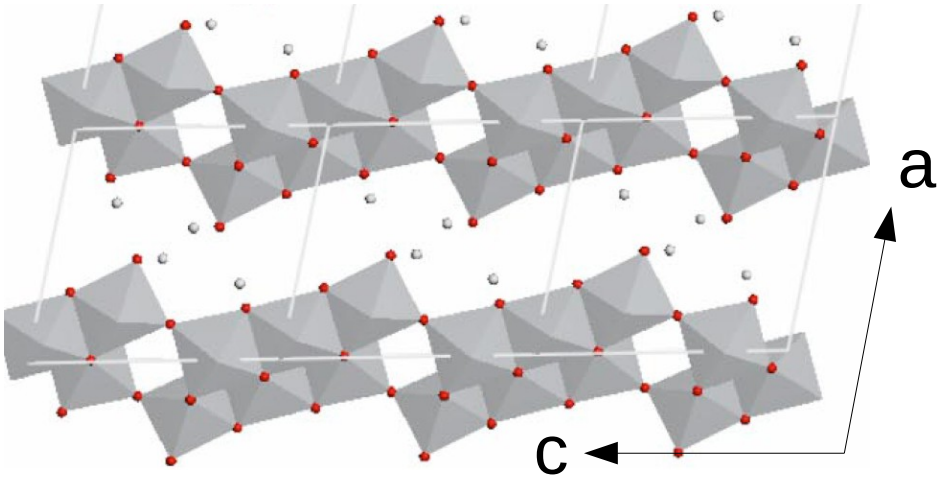

Bulk H2Ti3O7

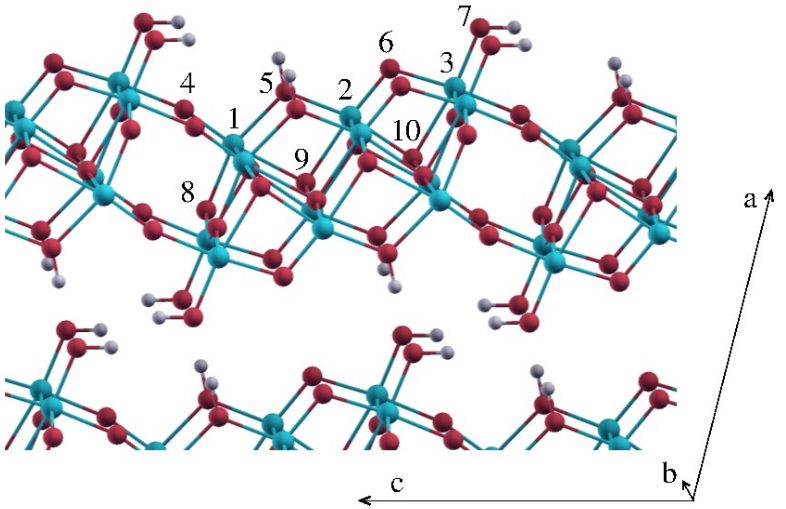

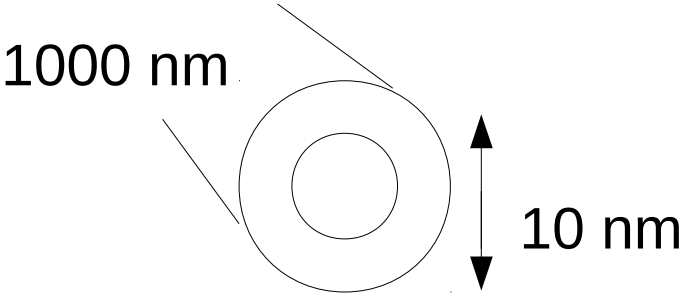

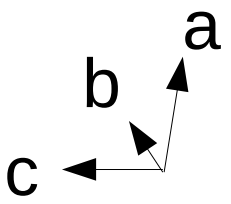

Structural model taken from S. Zhang et al, PRB 71, 014104 (2005)

TiO2 anatase: O-K edge XAS

Calculation: Density function theory, plane wave code (VASP)

O-K edge XAS ~ O-p projected Density of states ○ broadening function

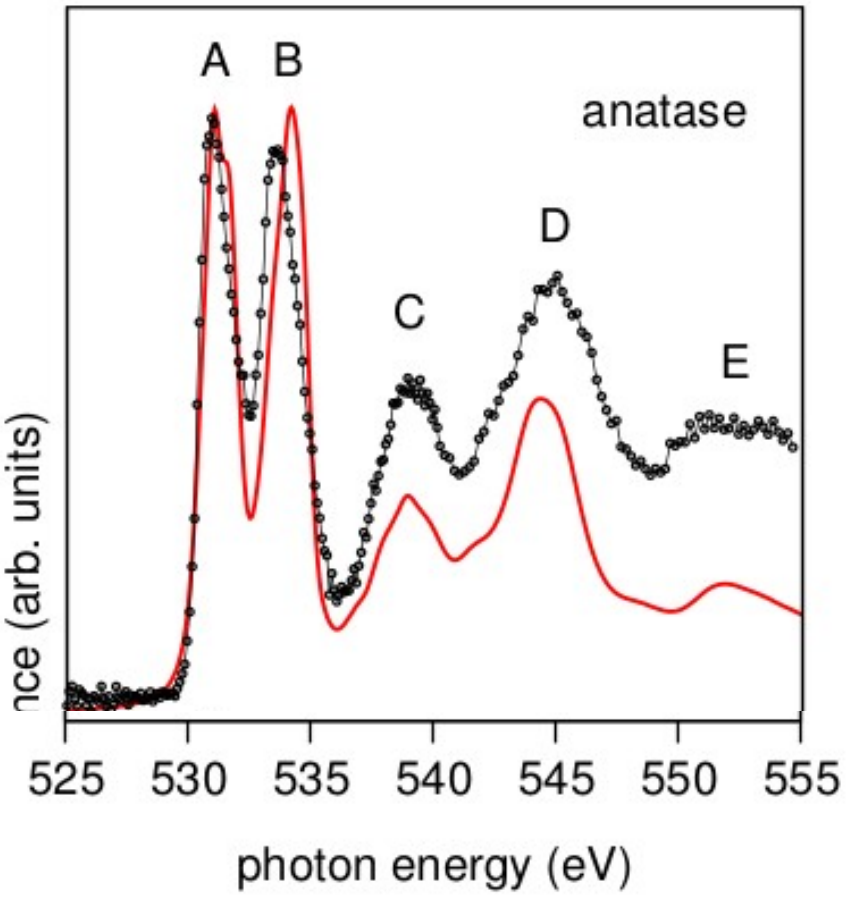

A -peak
T2g = pi-bond

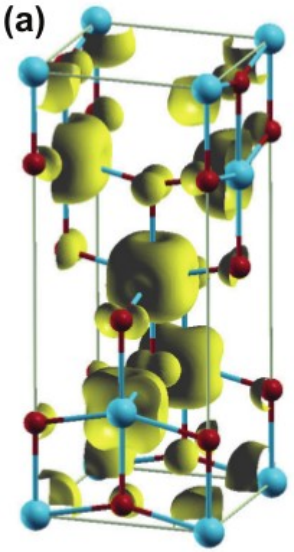

B -peak
Eg = sigma-bond

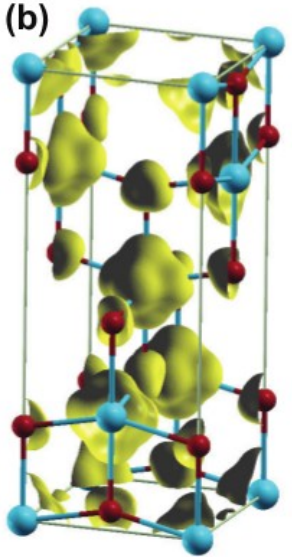

Nanotubes: O-K edge XAS

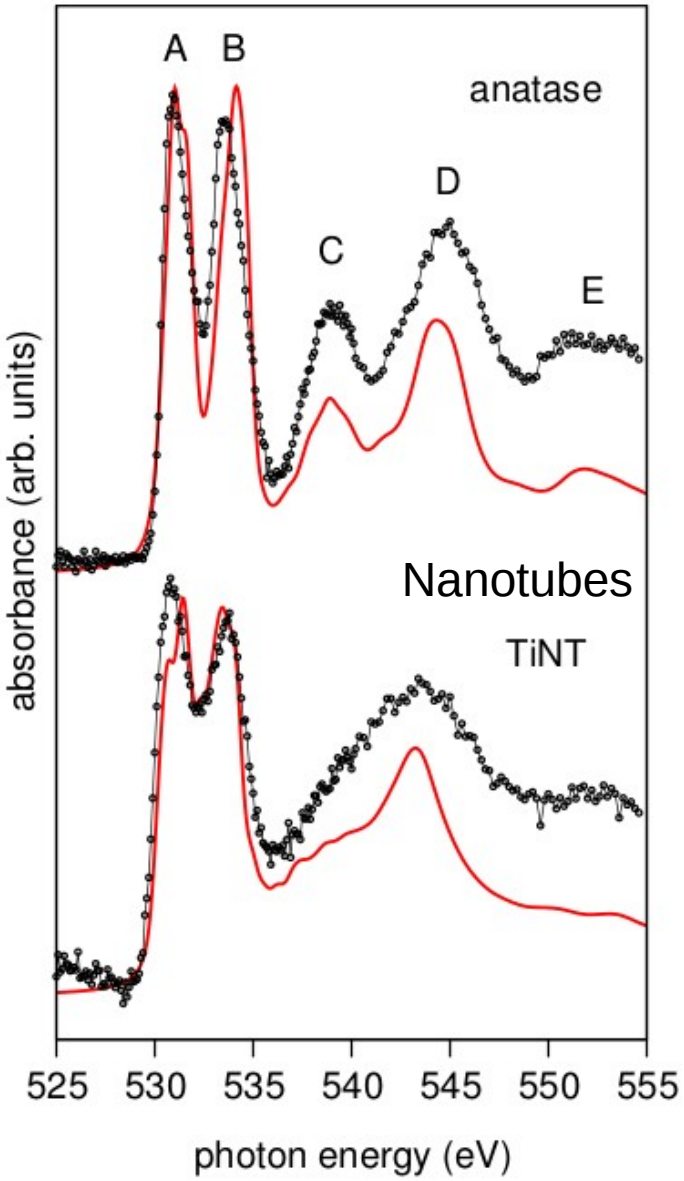

each O-site has individual spectral signature

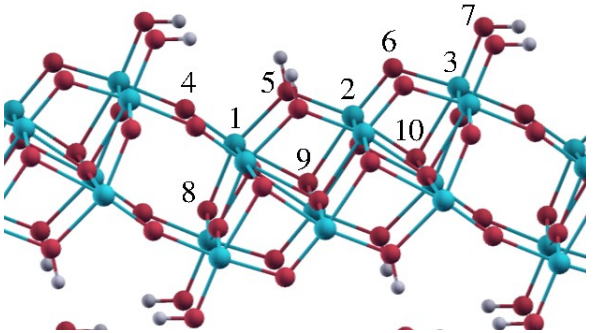

Nanotubes

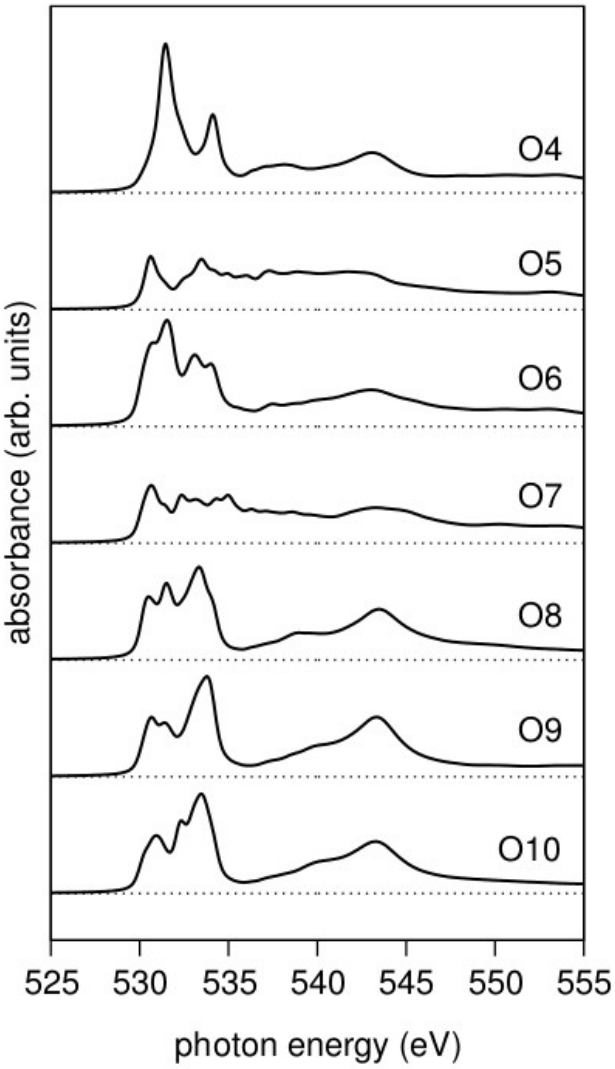

O-K edge XAS of nanotubes

B/A intensity increases with O-Ti coordination

→ B/A = local measure of connectivity of octahedra

O-Ti coordination = number of O-Ti sigma bonds

sigma bond → Ti-3d Eg orbital → B-peak

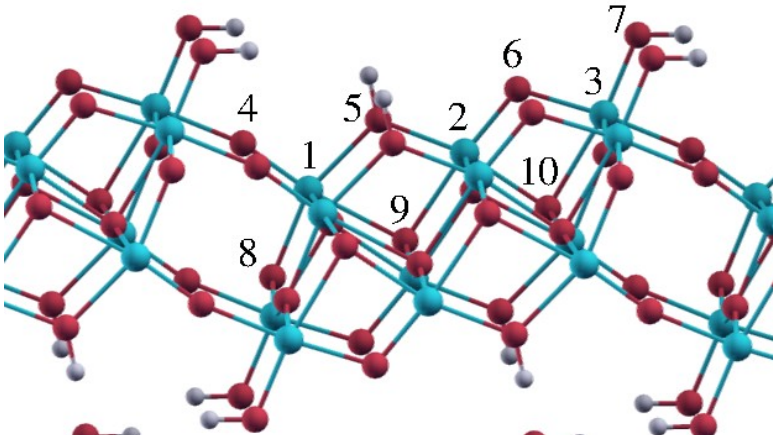

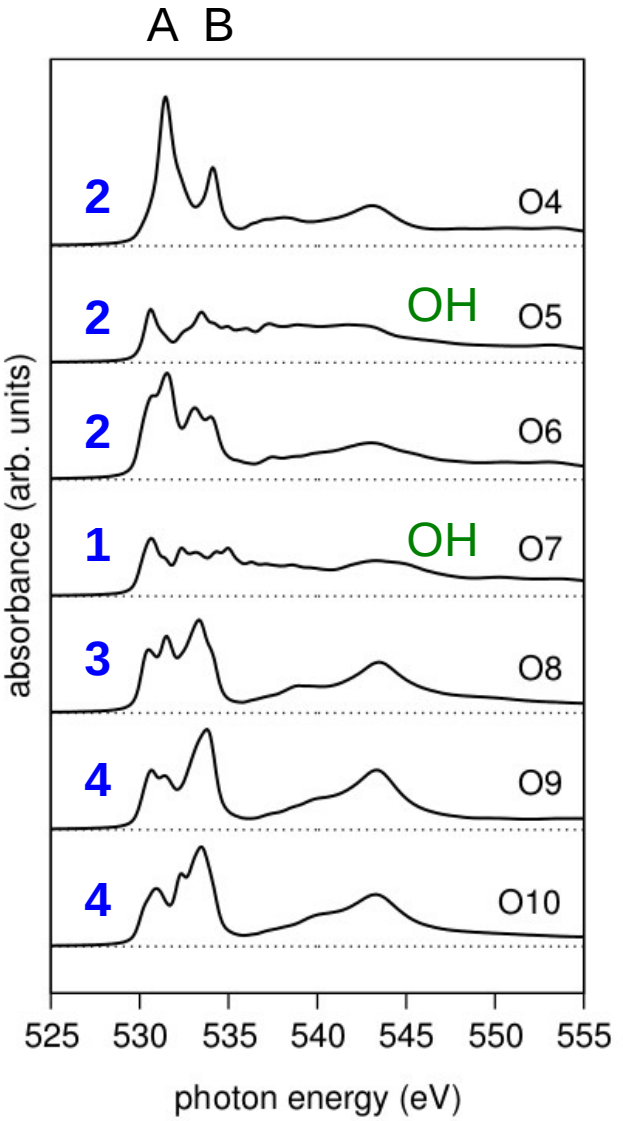

C. Bittencourt, PK et al, B.J.Nanotechnol.3, 789 (2012)

L23-edge spectra: TiO2

Final state multiplets →
all 1-electron schemes (DFT) fail

Instead:
multichannel multiple scattering
=
electron-hole multiplet coupling
(ab initio)
+
multiple scattering on big cluster
(300 atoms)

→ short and long range effects

→ spectra well reproduced for the 1st time

[P. Krüger, PRB 81, 125121 (2010)]

TiO_2 rutile

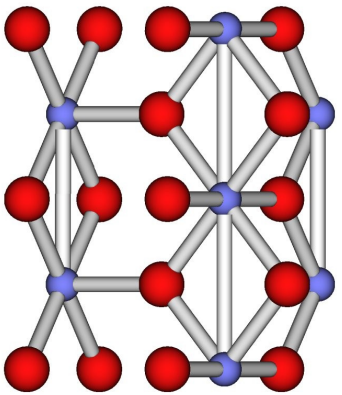

TiO_2 anatase

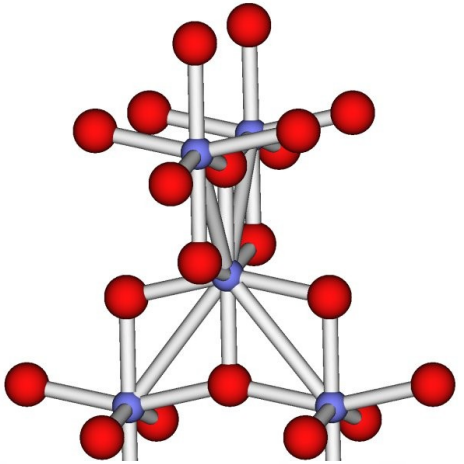

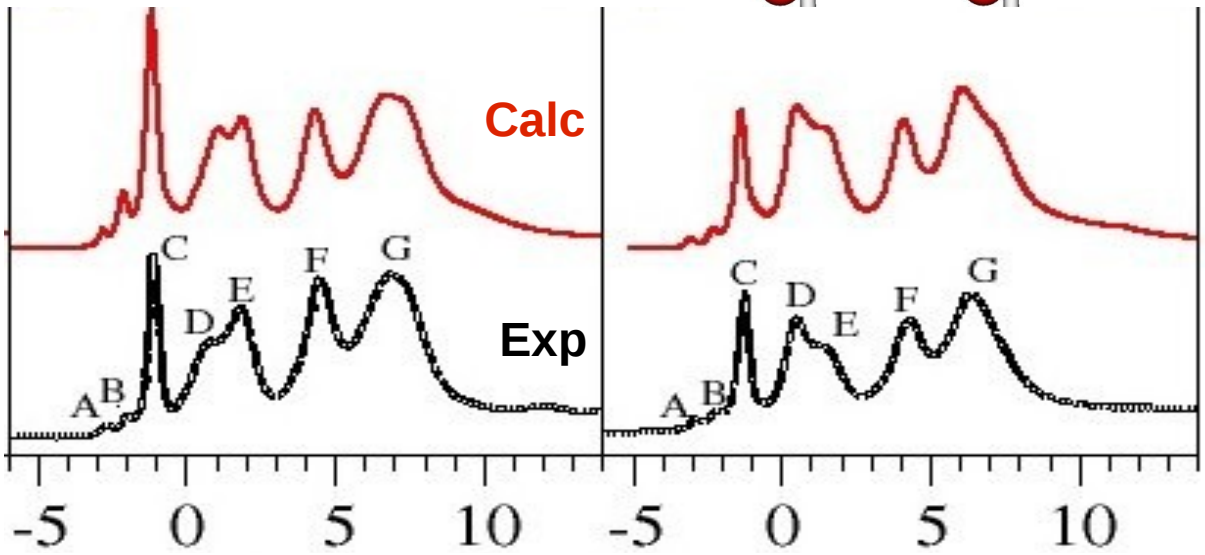

L23-edge XAS of TiO2 nanotubes

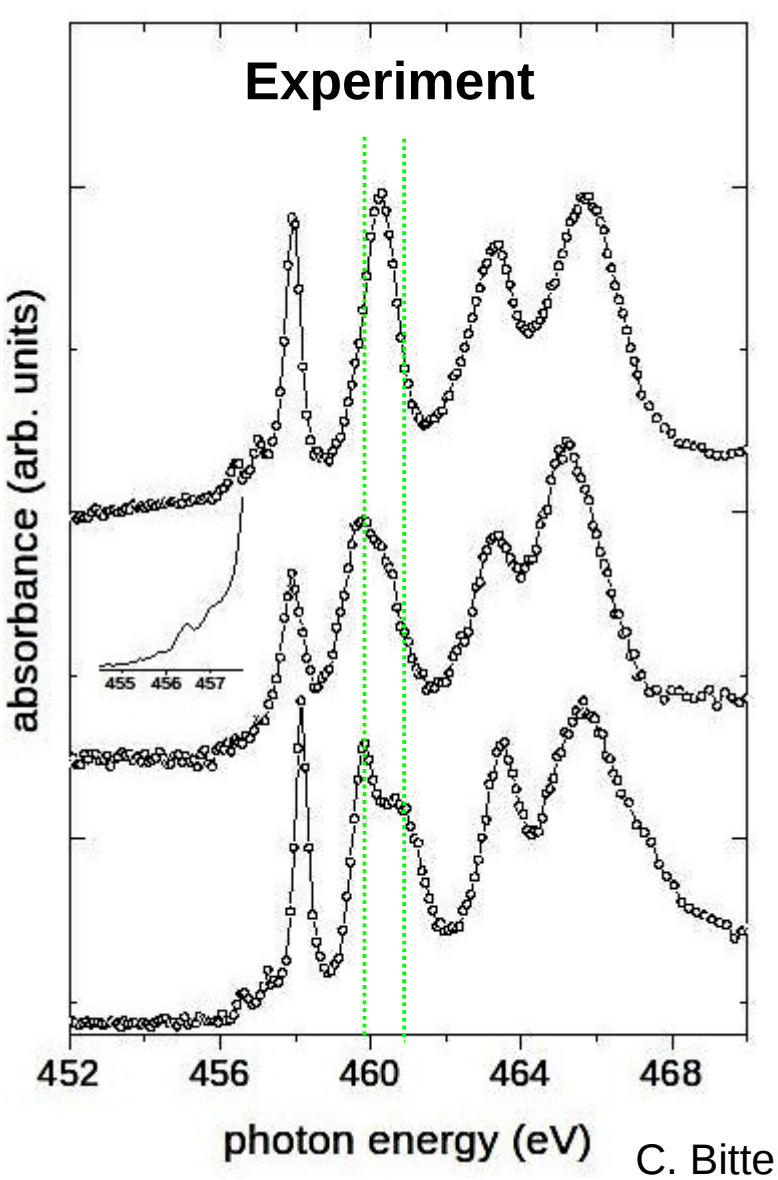

$SrTiO_3$

← **nanotubes** →

TiO_2
anatase

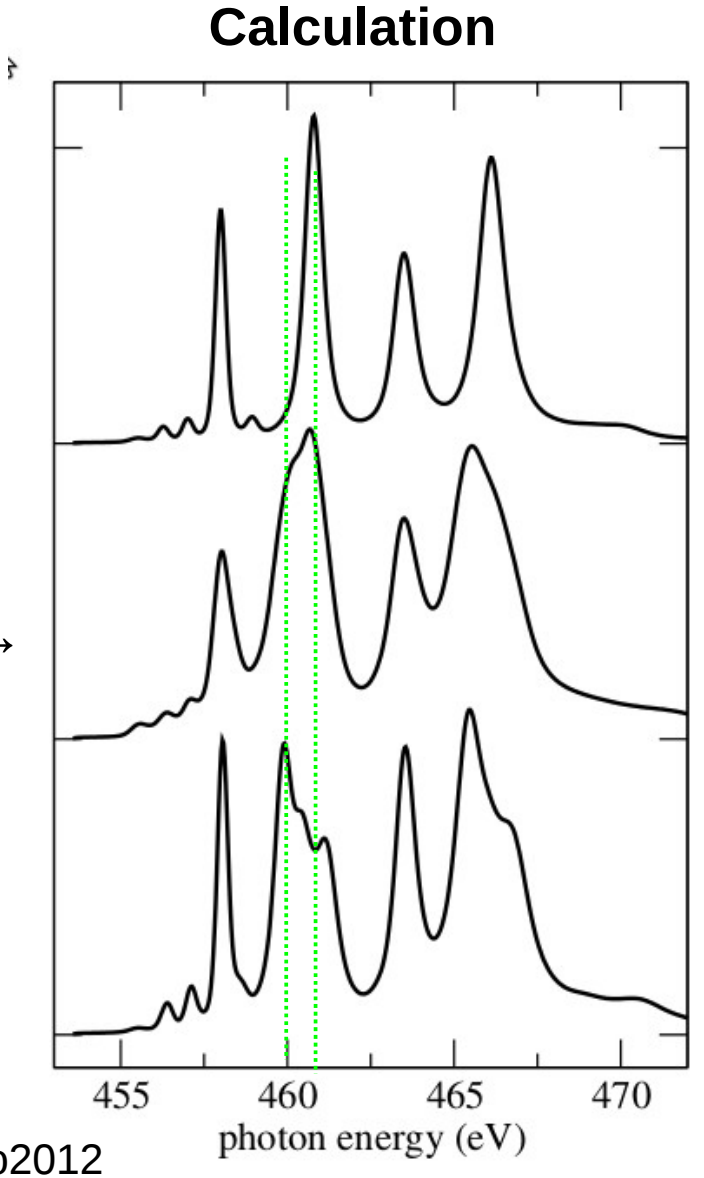

C. Bittencourt, PK et al, BJNano2012

D-E splitting

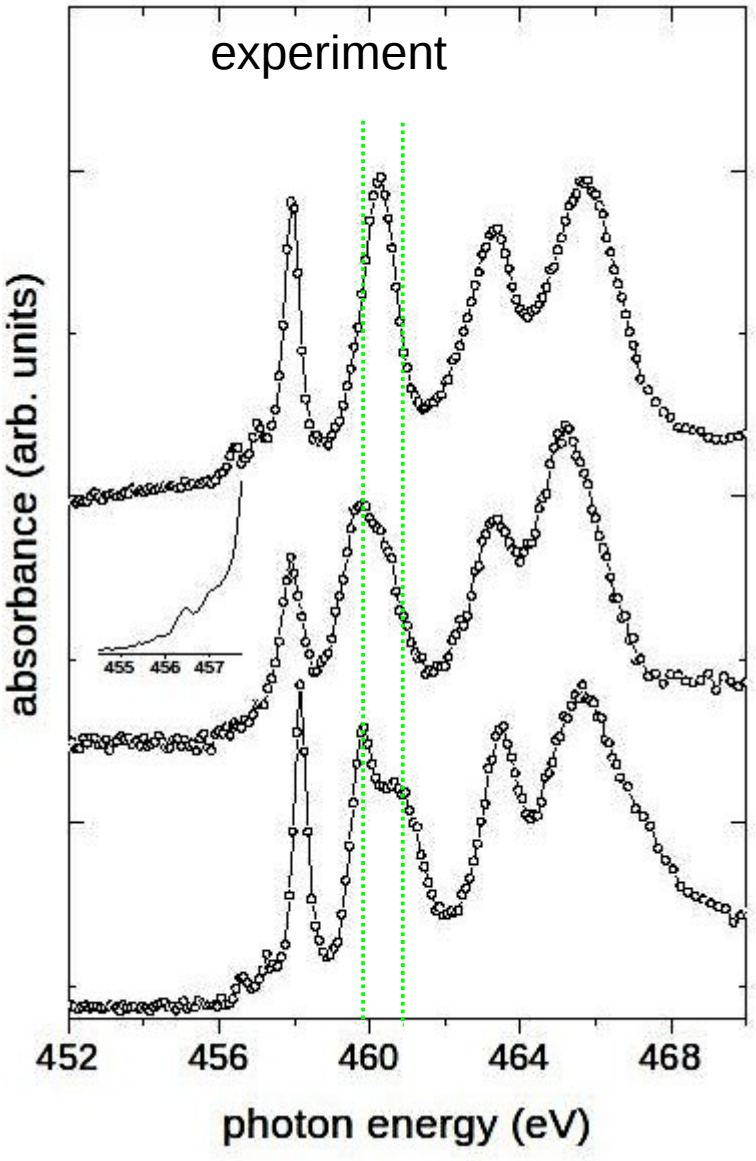

D-E splitting: TiO2 yes SrTiO3 no

connectivity of TiO6 octahedra

O-Ti coordination

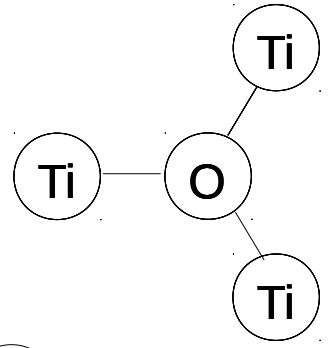

TiO2 3

SrTiO3 2

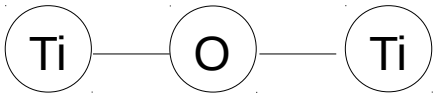

H2Ti3O7 2.6 (average)

D-E splitting
= rough mesure of O-Ti coordination
= number of edge shared octahedra

Nano-ribbons

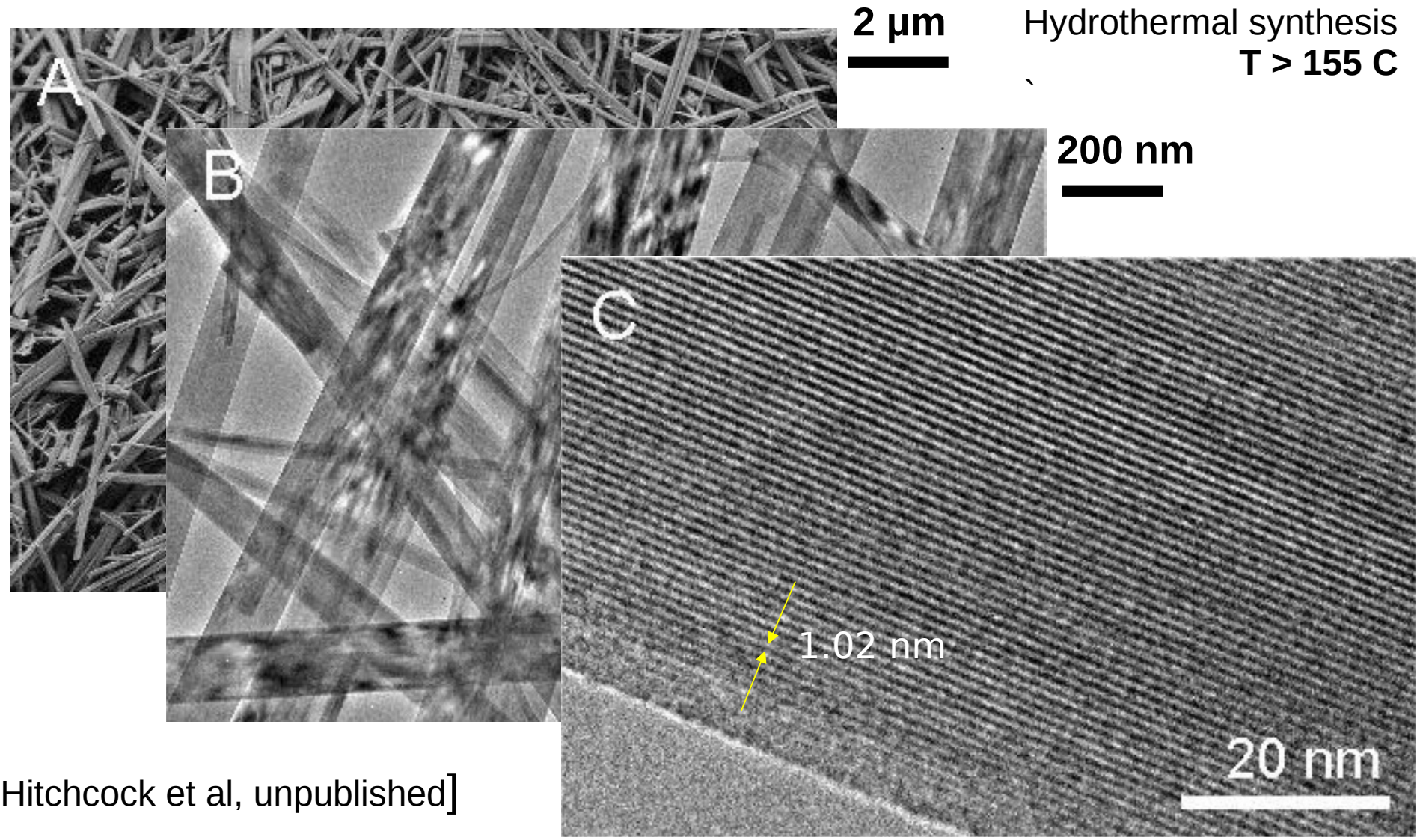

[A. Hitchcock et al, unpublished]

Structure of nanoribbons

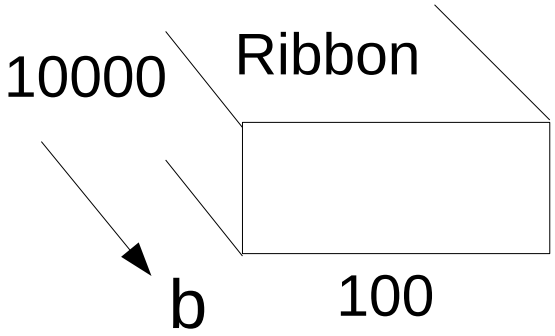

H2Ti3O7

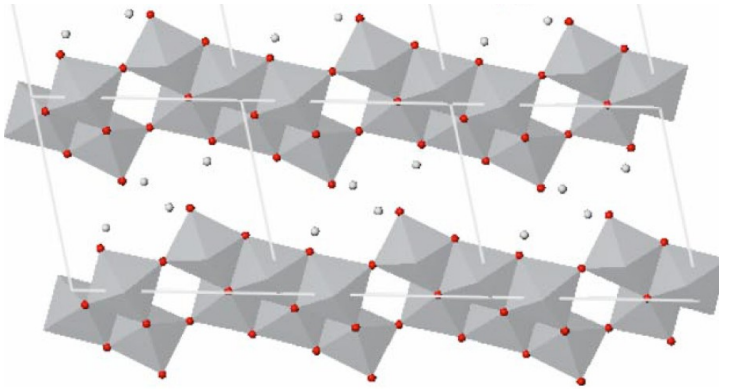

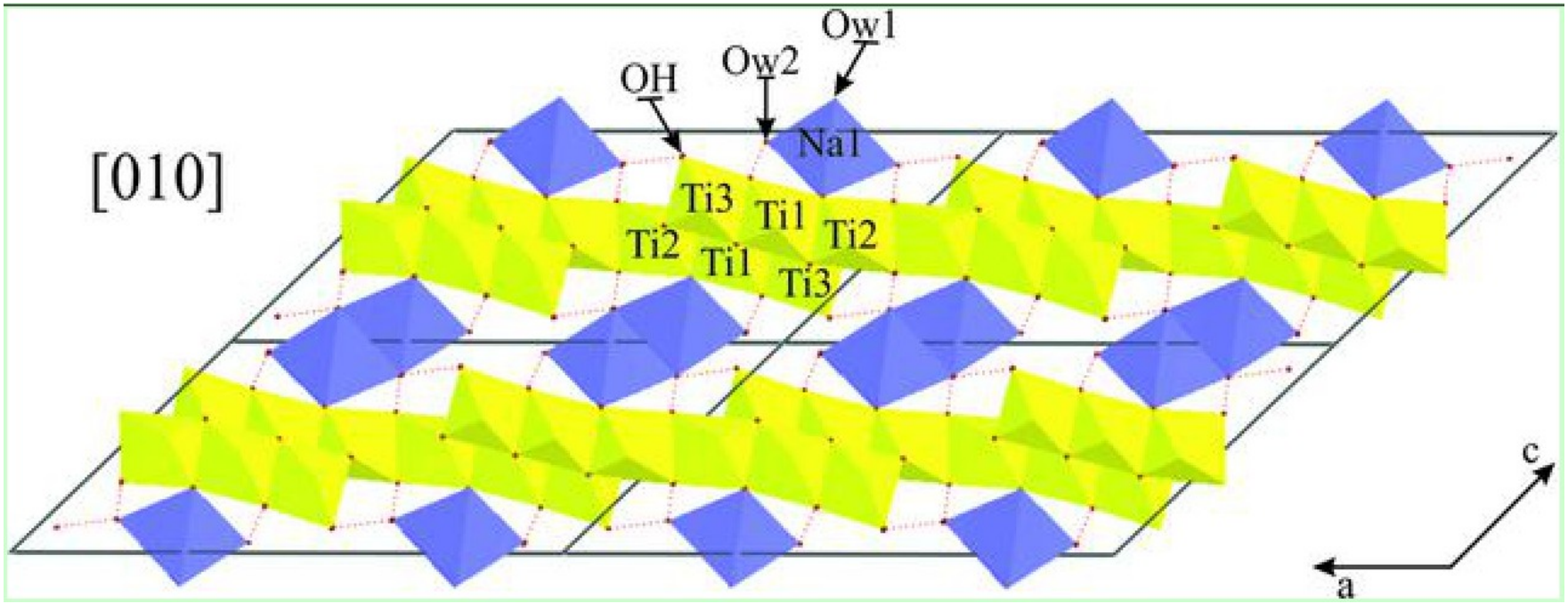

NaTi3O6(OH)x2H20.

I. Andrusenko et al. Acta Cryst. B 67 (2011) 218

NaTi3O6(OH)x2H20 Optimization

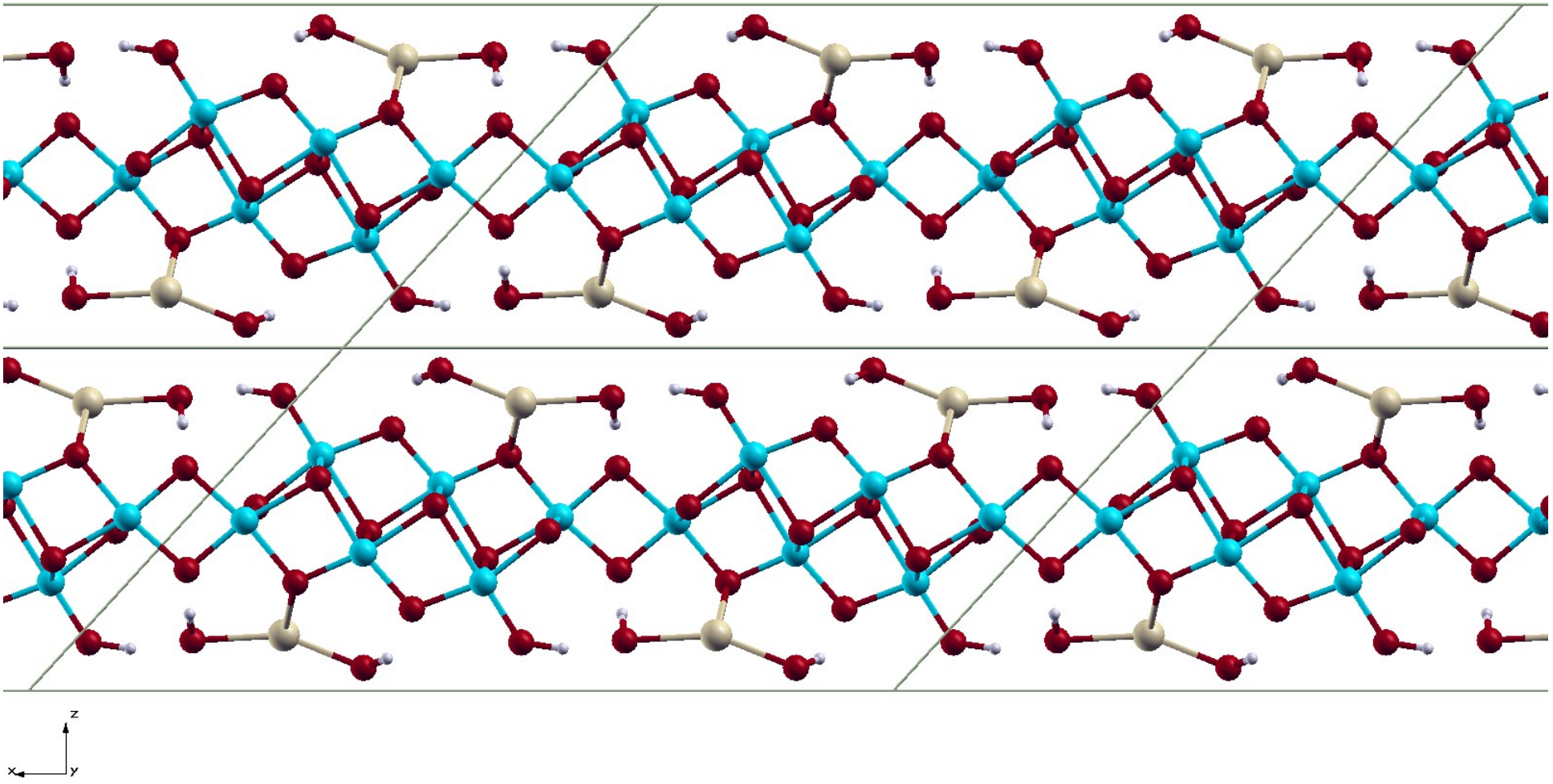

DFT-LDA optimized structure. Variance with exp: a=0.9%, b=0.1%, c=3.3%.
Hydrogen position agree with chemical insight (hydrogen bonds)

Nanoribbons: STXM

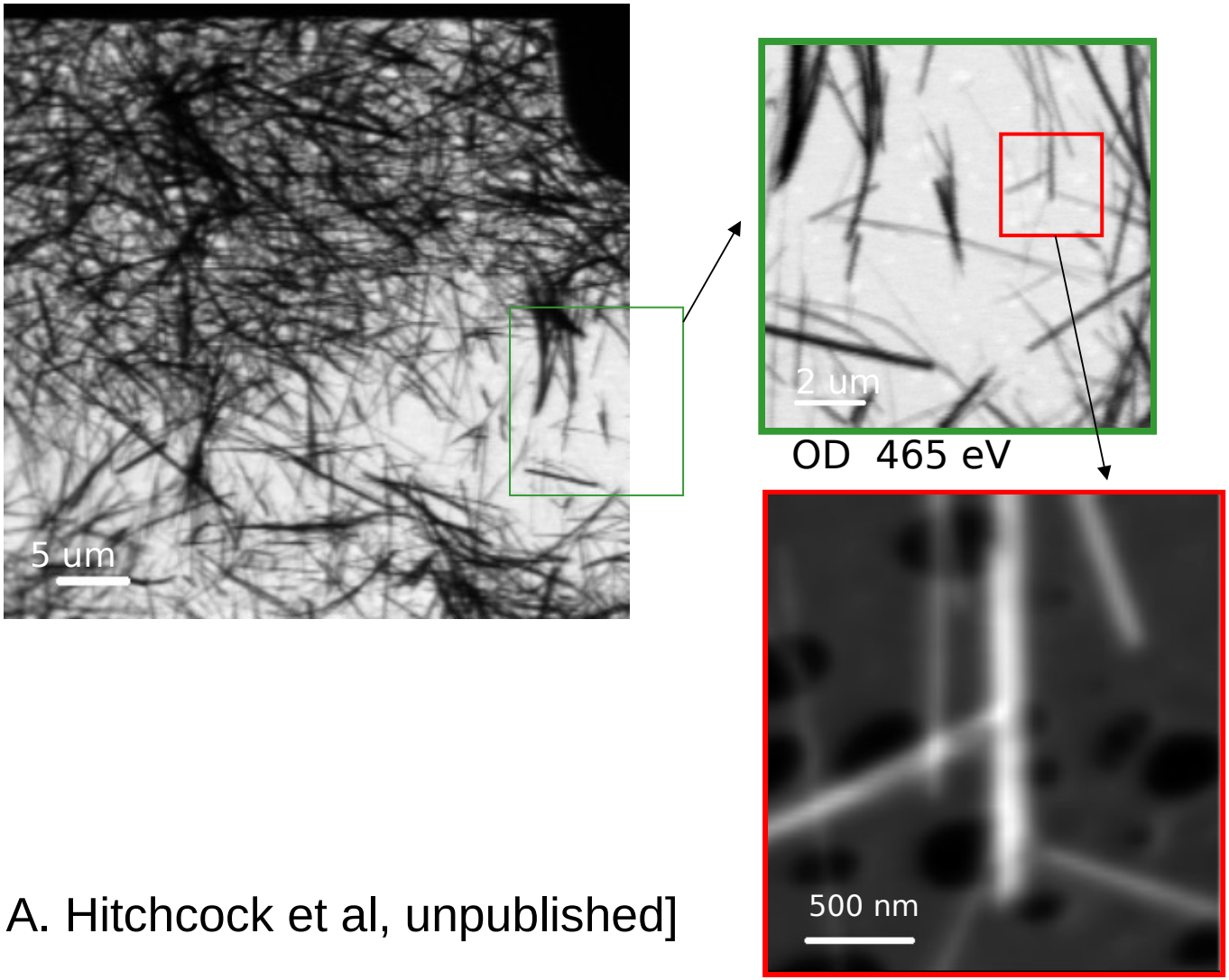

[X. Liu, A. Hitchcock et al, unpublished]

Nanoribbons: O-K edge dichroism

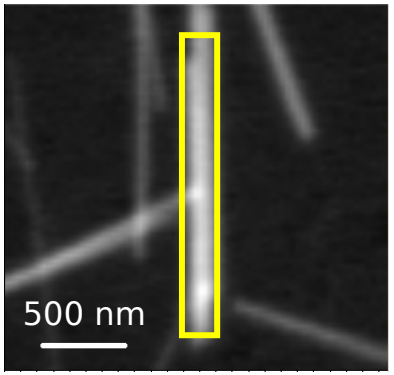

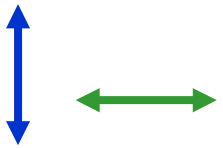

Polarization

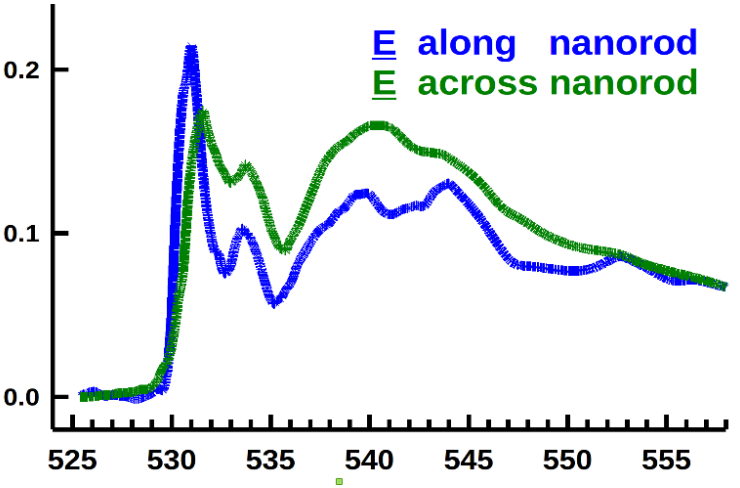

linear dichroism between along (**y**) and across (**x**,**z**) polarization

Experiment

H2Ti3O7

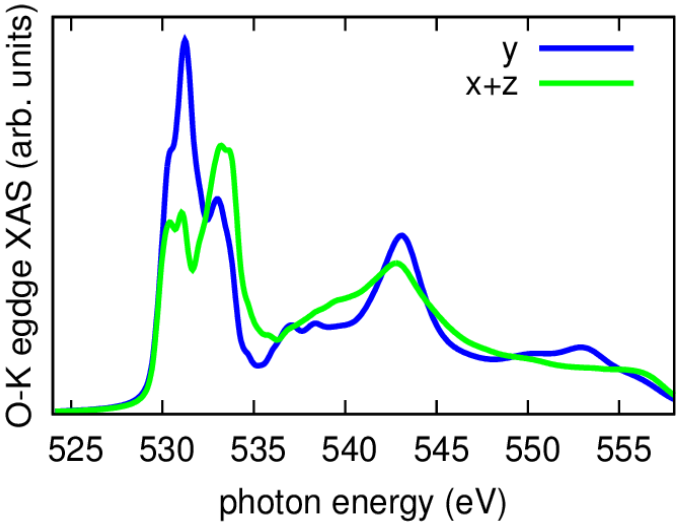

NaTi3O6(OH)x2H20

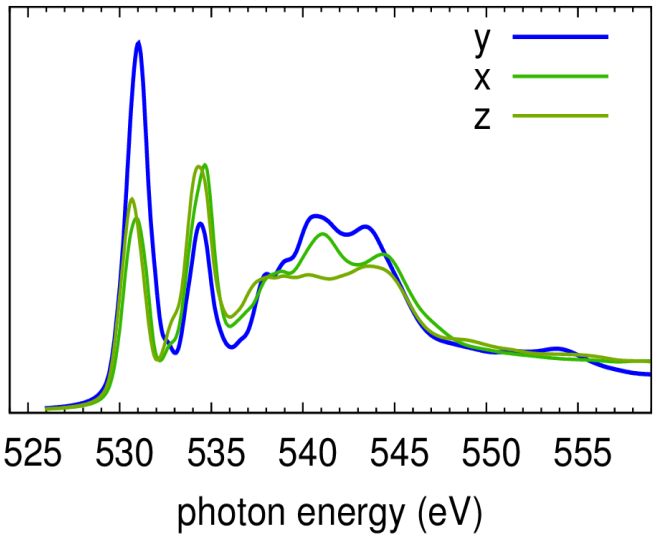

Calculation

good agreement

Origin of O-K edge dichroism

view along ribbons long axis (b)

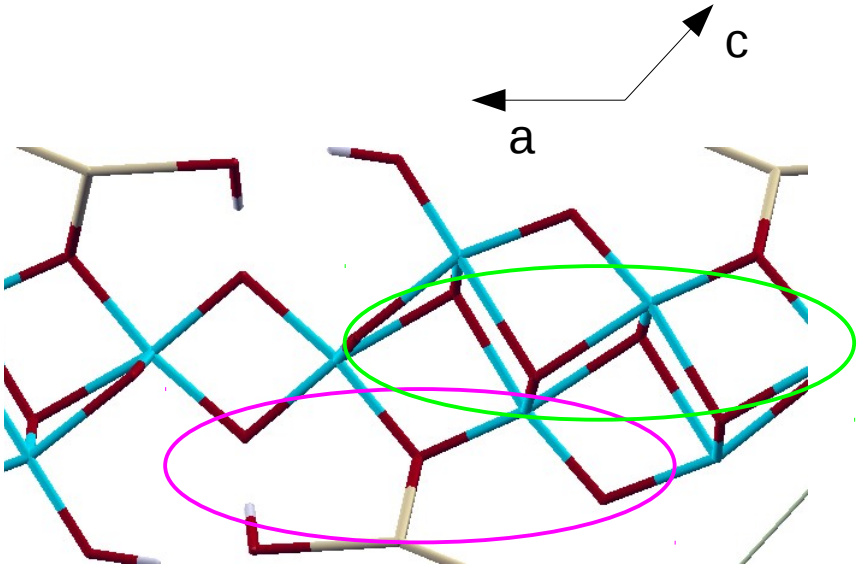

inner oxygens:
OTi4 ~ tetrahedrally coordinated
→ x,y,z equivalent → no dichroism

outer oxygen:
OTi2, all Ti-O bonds in (010) plane
Ti-O-Ti ~ right angle

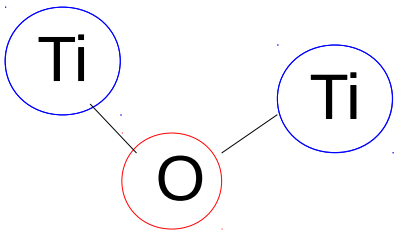

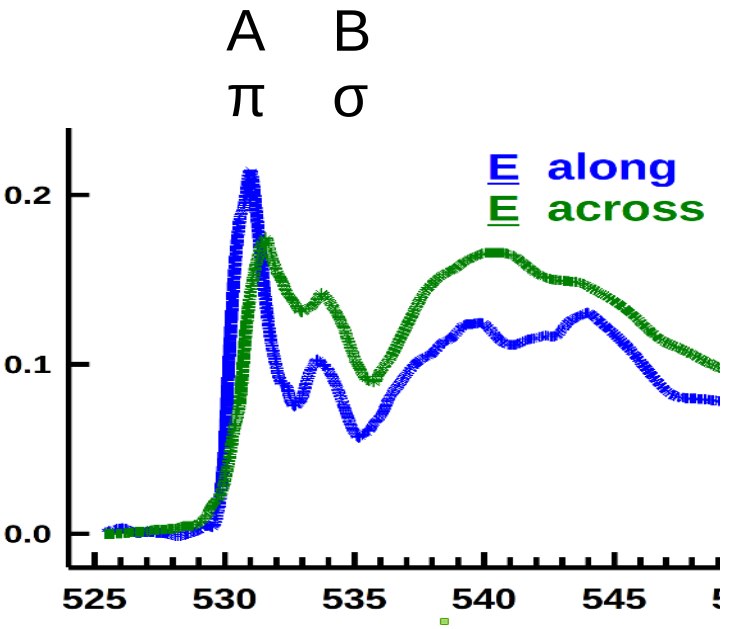

Origin of O-K dichroism

right angle Ti-O-Ti bond in xz plane

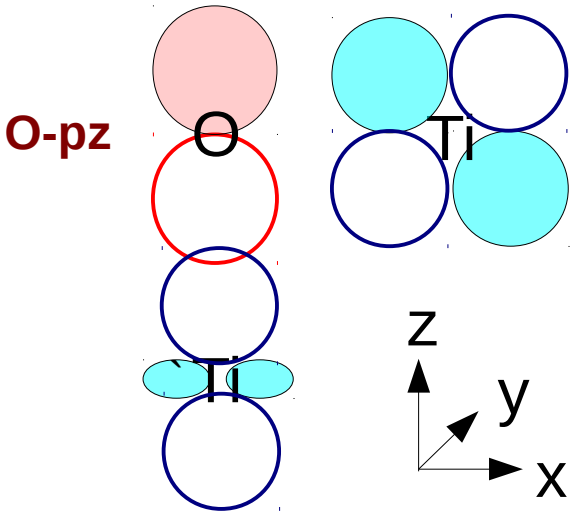

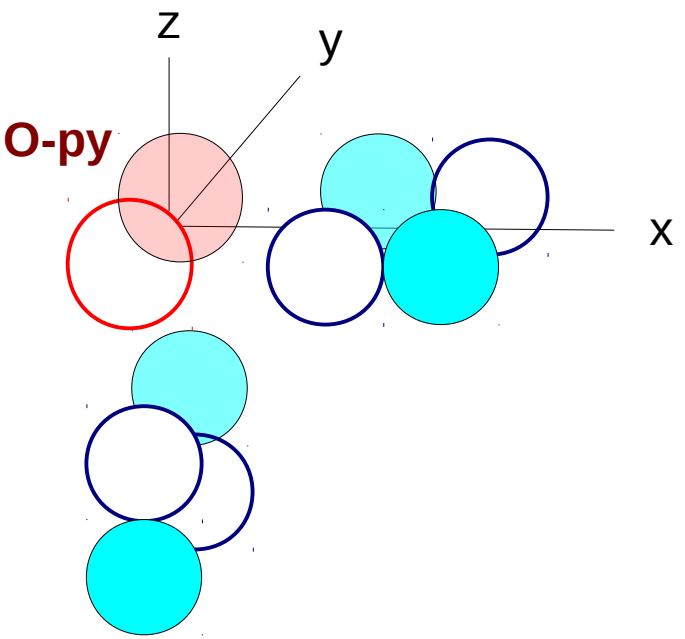

pz or px-orbital →

one π + one σ bond

py-orbital →

two π- bonds

Origin of O-K dichroism

Three inner O atoms:
→ no dichroism

Four outer O atoms:

in plane (ac)-plane polarisation
→ ½ σ + ½ π
↔ A peak ~B peak

out-of-plane (b) polarisation
→ π only
↔ A peak only

→ strong linear dichroism due to directional bonding of **outer** O atoms

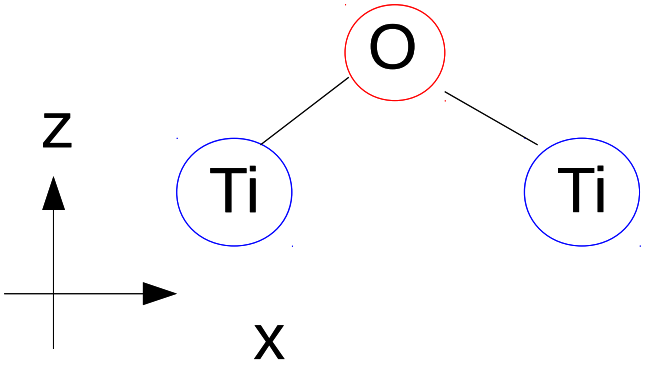

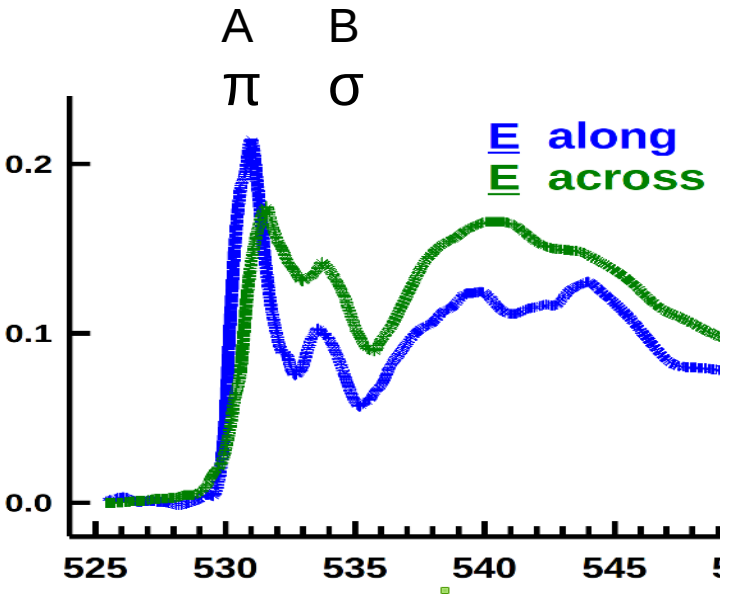

Nanoribbons: Ti-L23 edge dichroism

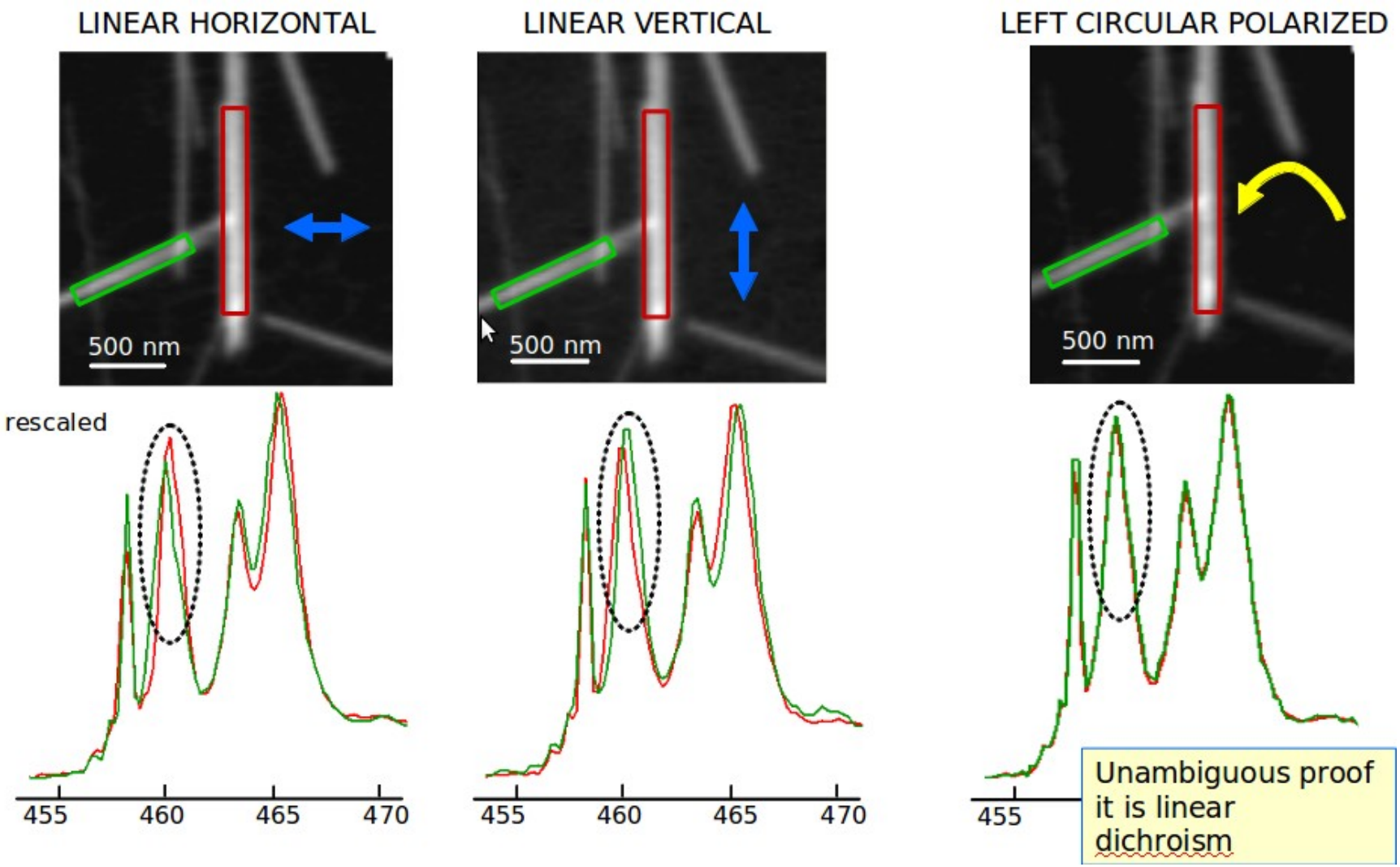

A. Hitchcock et al. (unpublished)

Nanoribbons: Ti-L23 edge dichroism

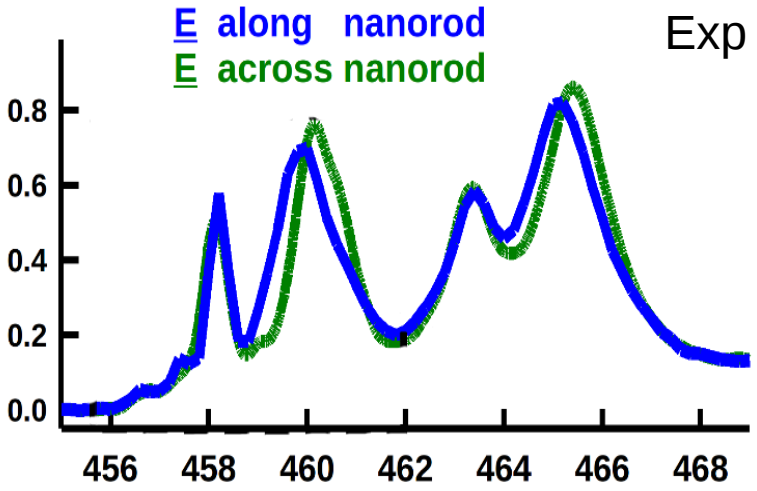

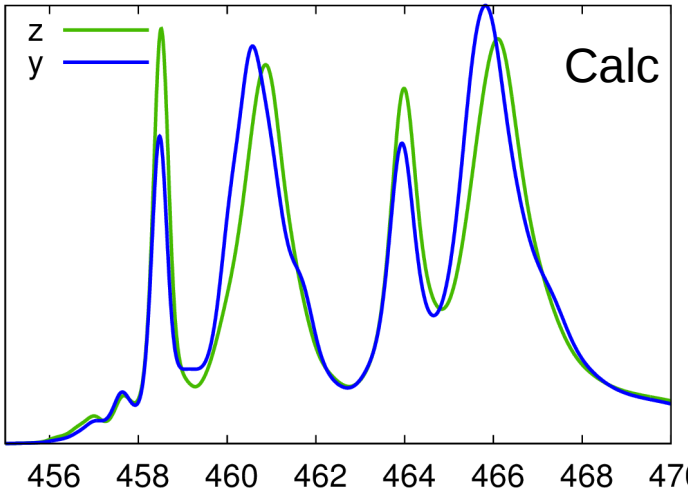

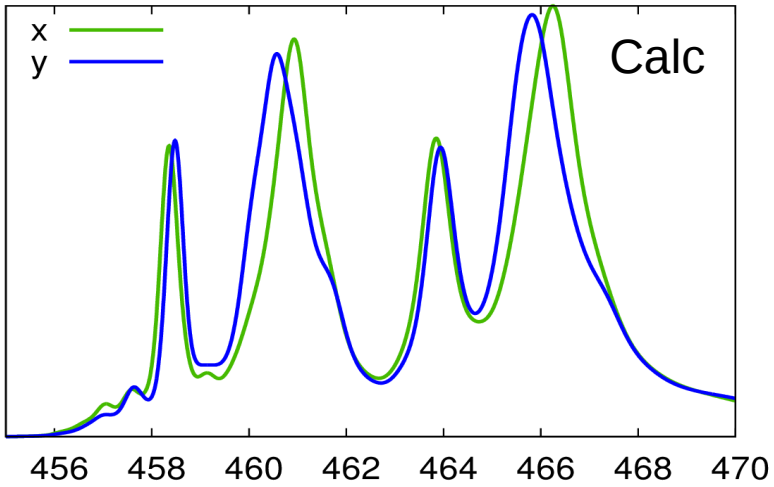

Calculation in multichannel theory
Ti 1,2,3 spectra aligned with experiment

Dichroism:

Eg-peak shift E(**along**) < E(**across**)

Calculation E(**y**) < E(**x,z**) agrees!

Conclusions

- Nanotubes:
  O-K A/B ratio = local measure of octahedra connectivity

- Nanoribbons:
  O-K dichroism: along/across rod ↔ π/σ bonds

- Ti-L23 edge well reproduced in multichannel theory, numerically light, nanostructures no problem

- First observation and first principles calculation of L23 edge dichroism in individual nanoparticles